



The effect of atmospheric CO₂ concentration on carbon isotope fractionation in C₃ land plants

Brian A. Schubert*, A. Hope Jahren

Department of Geology and Geophysics, University of Hawaii, Honolulu, HI 96822, USA

Received 30 November 2011; accepted in revised form 1 August 2012

Abstract

Because atmospheric carbon dioxide is the ultimate source of all land-plant carbon, workers have suggested that $p\text{CO}_2$ level may exert control over the amount of ^{13}C incorporated into plant tissues. However, experiments growing plants under elevated $p\text{CO}_2$ in both chamber and field settings, as well as meta-analyses of ecological and agricultural data, have yielded a wide range of estimates for the effect of $p\text{CO}_2$ on the net isotopic discrimination ($\Delta\delta^{13}\text{C}_p$) between plant tissue ($\delta^{13}\text{C}_p$) and atmospheric CO₂ ($\delta^{13}\text{C}_{\text{CO}_2}$). Because plant stomata respond sensitively to plant water status and simultaneously alter the concentration of $p\text{CO}_2$ inside the plant (c_i) relative to outside the plant (c_a), any experiment that lacks environmental control over water availability across treatments could result in additional isotopic variation sufficient to mask or cancel the direct influence of $p\text{CO}_2$ on $\Delta\delta^{13}\text{C}_p$. We present new data from plant growth chambers featuring enhanced dynamic stabilization of moisture availability and relative humidity, in addition to providing constant light, nutrient, $\delta^{13}\text{C}_{\text{CO}_2}$, and $p\text{CO}_2$ level for up to four weeks of plant growth. Within these chambers, we grew a total of 191 C₃ plants (128 *Raphanus sativus* plants and 63 *Arabidopsis thaliana*) across fifteen levels of $p\text{CO}_2$ ranging from 370 to 4200 ppm. Three types of plant tissue were harvested and analyzed for carbon isotope value: above-ground tissues, below-ground tissues, and leaf-extracted $n\text{C}_{31}$ -alkanes. We observed strong hyperbolic correlations ($R \geq 0.94$) between the $p\text{CO}_2$ level and $\Delta\delta^{13}\text{C}_p$ for each type of plant tissue analyzed; furthermore the linear relationships previously suggested by experiments across small (10–350 ppm) changes in $p\text{CO}_2$ (e.g., 300–310 ppm or 350–700 ppm) closely agree with the amount of fractionation per ppm increase in $p\text{CO}_2$ calculated from our hyperbolic relationship. In this way, our work is consistent with, and provides a unifying relationship for, previous work on carbon isotopes in C₃ plants at elevated $p\text{CO}_2$. The values for $\Delta\delta^{13}\text{C}_p$ we determined in our ambient $p\text{CO}_2$ chambers are consistent with the $\Delta\delta^{13}\text{C}_p$ values measured in large modern datasets of plants growing within the Earth's wettest environments, suggesting that it may be possible to reconstruct changes in paleo- $p\text{CO}_2$ level from plants that grew in consistently wet environments, if $\delta^{13}\text{C}_{\text{CO}_2}$ value and initial $p\text{CO}_2$ level can be independently quantified. Several implications arise for the reconstruction of water availability and water-use efficiency in both ancient and recent plant $\Delta\delta^{13}\text{C}_p$ values across periods of changing $p\text{CO}_2$ level. For example, the change in $\Delta\delta^{13}\text{C}_p$ implied by our relationship for the rise in $p\text{CO}_2$ concentration observed since 1980 is of the same magnitude ($\approx 0.7\text{‰}$) as the isotopic correction for changes in $\delta^{13}\text{C}_{\text{CO}_2}$ required by the input of ^{13}C -depleted carbon to the atmosphere. For these reasons, only the portion of the terrestrial isotopic excursion that persists after accounting for changes in $p\text{CO}_2$ concentration should be used for the interpretation of a change in paleo-environmental conditions.

© 2012 Elsevier Ltd. All rights reserved.

1. INTRODUCTION

Because carbon dioxide is a raw material for photosynthesis, the $p\text{CO}_2$ level of the atmosphere ultimately represents the availability of carbon for land-plant growth. Many studies have demonstrated the influence of increasing

* Corresponding author. Tel.: +1 808 956 0457; fax: +1 808 956 5512.

E-mail address: bschube@hawaii.edu (B.A. Schubert).

$p\text{CO}_2$ on plant growth (Hunt et al., 1991, 1993; Kimball et al., 1993; Poorter, 1993; Ceulemans and Mousseau, 1994; Wand et al., 1999; Poorter and Navas, 2003; Ainsworth and Long, 2005; Schubert and Jahren, 2011) and on various plant functions, including increased CO_2 -assimilation rate (Figure. 1.5 within Fitter and Hay, 2002), short-term decreased photosynthetic rate (Greer et al., 1995), increased seedling growth (Bazzaz, 1974), decreased nitrogen-content in leaves (Figure 14.4 within Bazzaz, 1996), decreased stomatal density (Woodward, 1987; Woodward and Bazzaz, 1988; Woodward and Kelly, 1995; Royer, 2001), and increased intrinsic water-use efficiency (Waterhouse et al., 2004; Gagen et al., 2011). These changes carry implications at the ecosystem level, such that increased $p\text{CO}_2$ implies changes in competition (Hunt et al., 1993), succession of species (Condon et al., 1992; Mousseau and Saugier, 1992; Bazzaz and Miao, 1993), decomposition rates (Melillo et al., 1982; Norby et al., 2001), and reproduction (Downton et al., 1987; Andersson, 1991).

Plant tissues exhibit a ^{13}C -depleted isotopic signature relative to the atmosphere because ^{12}C is preferentially selected for fixation over ^{13}C as CO_2 is converted to sugar within leaves (Park and Epstein, 1960). Within C_3 plants (i.e., plants that employ only the RuBisCO enzyme to catalyze CO_2 fixation), the net isotopic difference between the atmospheric CO_2 and the resultant plant tissue has been modeled according to the following equation (Farquhar et al., 1989):

$$\Delta\delta^{13}\text{C}_p = a + (b - a)(c_i/c_a) \quad (1)$$

where

$$\Delta\delta^{13}\text{C}_p = (\delta^{13}\text{C}_{\text{CO}_2} - \delta^{13}\text{C}_p) / (1 + \delta^{13}\text{C}_p/1000) \quad (2)$$

Within the above, the constants a and b represent the isotopic fractionation due to diffusion through the plant's stomata and subsequent catalysis by RuBisCO, respectively; $\delta^{13}\text{C}_p$ and $\delta^{13}\text{C}_{\text{CO}_2}$ are the carbon isotope composition of plant tissue and CO_2 in the atmosphere, respectively. Due to the combined action of both diffusion and fixation, the intracellular concentration of CO_2 (c_i) is less than the atmospheric concentration of CO_2 (c_a). Because a land plant's main mechanism of responding to environmental conditions is by closing or opening stomata, variation in $\delta^{13}\text{C}_p$ is often interpreted as a change in c_i caused by a change in stomatal conductance. Indeed, many environmental characteristics known to directly affect stomatal aperture have been shown to be correlated with $\delta^{13}\text{C}_p$ [e.g., water availability (Warren et al., 2001), precipitation (Diefendorf et al., 2010; Kohn, 2010), relative humidity (Farquhar et al., 1982), and soil moisture content (Ehleringer and Cooper, 1988)]. This has led workers to adopt the interpretation of (c_i/c_a) as a measure of water-use efficiency (Farquhar and Richards, 1984; Farquhar et al., 1988). Other environmental characteristics that may have an indirect affect on stomatal aperture (e.g., through a generalized stress response) have also been observed to correlate with $\delta^{13}\text{C}_p$ [e.g., nutrient availability (Warren et al., 2001), air pollutants (Martin et al., 1988; Savard, 2010), and soil salinity (Lin and Sternberg, 1992)]. The effect of temperature on $\delta^{13}\text{C}_p$ has remained inconsistent,

as both positive and negative correlations are commonly reported (Körner et al., 1991; Gröcke, 1998; Schleser et al., 1999; McCarroll and Loader, 2004; Daux et al., 2011).

Because atmospheric $p\text{CO}_2$ has been shown to influence multiple aspects of plant biology, workers have hypothesized that changes in $p\text{CO}_2$ level may directly influence $\Delta\delta^{13}\text{C}_p$ (Ehleringer and Cerling, 1995; Beerling, 1996; Beerling and Royer, 2002; Tcherkez et al., 2006), but the magnitude of this response is uncertain. While records of $\Delta\delta^{13}\text{C}_p$ in modern wood have recently been reported to show a positive correlation with increasing $p\text{CO}_2$ over the last 160 years (Gagen et al., 2007; Kirilyanov et al., 2008; Loader et al., 2008; McCarroll et al., 2009; Treydte et al., 2009), early meta-analysis of published data revealed no correlation with $p\text{CO}_2$ (Fig. 1 within Arens et al., 2000). In addition, multiple studies of $\Delta\delta^{13}\text{C}_p$ have been performed upon plants growing across a gradient of $p\text{CO}_2$ level, either in growth chambers (Beerling and Woodward, 1995; Jahren et al., 2008; Schubert and Jahren, 2011) or in field experiments (Saurer et al., 2003; Sharma and Williams, 2009); other workers have attempted to correlate past $p\text{CO}_2$ level with the $\Delta\delta^{13}\text{C}_p$ values of sub-fossil tree rings (Feng and Epstein, 1995; Berninger et al., 2000; Hietz et al., 2005; McCarroll et al., 2009; Treydte et al., 2009; Wang et al., 2011) and fossil leaves (Beerling et al., 1993; Beerling and Woodward, 1993; Van de Water et al., 1994; Beerling, 1996; Peñuelas and Estiarte, 1997). The majority of these modern and fossil studies show a positive correlation between $\Delta\delta^{13}\text{C}_p$ and $p\text{CO}_2$ (Beerling et al., 1993; Van de Water et al., 1994; Beerling and Woodward, 1995; Kürschner et al., 1996; Peñuelas and Estiarte, 1997; Berninger et al., 2000; Saurer et al., 2003; Hietz et al., 2005; Sharma and Williams, 2009; Treydte et al., 2009); however, negative correlation (Beerling and Woodward, 1993; Beerling, 1996) and no correlation (Jahren et al., 2008) have also been reported. Therefore, there exists no clear consensus as to the effect that $p\text{CO}_2$ has on $\Delta\delta^{13}\text{C}_p$. However, the above laboratory and field experiments generally lack constant environmental control (especially water availability) across treatments, therefore any direct influence of $p\text{CO}_2$ on $\Delta\delta^{13}\text{C}_p$ could have been masked or canceled by variation in c_i conferred by the multiple direct and indirect effects of environmental heterogeneity on stomatal conductance. Here, we report new data from laboratory experiments conducted within growth chambers featuring enhanced dynamic stabilization of moisture availability and relative humidity, as well as providing constant light, nutrient, $\delta^{13}\text{C}_{\text{CO}_2}$, and $p\text{CO}_2$ level throughout up to four weeks of plant growth. These experiments, conducted across a wide range of $p\text{CO}_2$ levels while maintaining control over environmental characteristics, yielded new insight into the quantitative effect of $p\text{CO}_2$ level on C_3 land-plant $\Delta\delta^{13}\text{C}_p$ values.

2. METHODS

2.1. Experimental methods

We grew a total of 128 *Raphanus sativus* plants and 63 *Arabidopsis thaliana* (both C_3 plants) under controlled

growth conditions. All plant growth occurred within (0.51 cubic meter) positive-pressure Plexiglass chambers designed to control light levels, temperature, relative humidity, $p\text{CO}_2$ level, and $\delta^{13}\text{C}_{\text{CO}_2}$ within the growth environment (after Jahren et al., 2008; Schubert and Jahren, 2011)(Fig. 1, Tables EA1-EA2). The growth chambers were placed within a $7.32 \times 3.66 \times 2.74$ m air-conditioned room maintained at 20°C . Photosynthetic photon flux was maintained at $260 \mu\text{mol m}^{-2} \text{s}^{-1}$ (400–700 nm) using adjustable fluorescent grow lamps (33-W GE Brightstik); light levels were measured daily at the leaf surface using a Solar Electric Quantum Meter (Spectrum Technologies, Inc.) in conjunction with a diurnal timer which provided 11.75 h (*R. sativus*) and 11.00 h (*A. thaliana*) of continuous light per 24-h cycle. All *A. thaliana* plants were maintained at $24.8 \pm 0.4^\circ\text{C}$ (average $\pm 1\sigma$), which is within the ideal temperature range of this model organism (Kipp, 2008); half the *R. sativus* plants were grown at $25.6 \pm 1.0^\circ\text{C}$ and half at $30.3 \pm 1.4^\circ\text{C}$ in order to cover the range of temperatures shown for maximum growth of *R. sativus* (Fig. 2 within Idso and Kimball, 1989). Two temperature regimes were obtained for *R. sativus* by arranging the experiments vertically within the chambers, which allowed for heat to rise from the lower experiment to the higher. Each plant occupied a separate soil container and was supplied with excess nitrogen, phosphorous, and trace nutrients. Soil was watered twice daily to maintain field-moist conditions as defined by the Soil Survey Staff and Soil Conservation Service (1999) through a manually-operated drip system. By dynamically stabilizing temperature, light, and soil moisture, we were able to maintain daytime relative humid-

ity at $39 \pm 6\%$ for the duration of all experiments (measured using Fisher Scientific Humidity Monitor, model #06-662-4). As expected, the necessary water delivery to the plants was variable in order to maintain constant soil moisture and relative humidity for the period of growth. Within the *R. sativus* experiments, plants grown at the higher temperature required significantly more water than plants grown at the cooler temperature ($P = 0.003$). *A. thaliana* plants overall required significantly less water than the *R. sativus* plants ($P < 0.0001$), which we attributed to the $\sim 11.5\times$ greater (above-ground) biomass of *R. sativus* over *A. thaliana* for plants grown under ambient $p\text{CO}_2$.

Fifteen different $p\text{CO}_2$ levels were used for growth ($n = 8$, *R. sativus*; $n = 7$, *A. thaliana*) ranging between 370 and 4200 ppm in order to span the full range of $p\text{CO}_2$ levels estimated for the Phanerozoic (Berner, 2006; Breecker et al., 2010). Carbon dioxide levels were increased by bleeding pure cylinder CO_2 into an intake pipe where it mixed with ambient air before reaching the growth chamber. Air was exhausted through an upper pipe and vented through a fume hood; a fan within the intake pipe maintained the chamber at positive pressure; complete atmospheric turnover occurred approximately once every 10.4 min. For each chamber the CO_2 flow rate was precisely controlled with an inline micro-control valve (SGE Analytical Science, #1236012) at the pure CO_2 source in order to maintain constant $p\text{CO}_2$ levels (confirmed using a Telaire 7001 carbon dioxide and temperature monitor). The average $p\text{CO}_2$ levels for each of the eight *R. sativus* experiments were 407, 497, 576, 780, 1494, 2723, 3429, and 4200 ppm; the seven *A. thaliana* experiments were conducted at $p\text{CO}_2$ levels of 370, 455, 733, 995, 1302, 1843, and 2255 ppm.

We chose to grow *A. thaliana* based on recent reports of its growth at 550 ppm (Li et al., 2008) and the wealth of previous biological characterizations based on its use as the genome-based molecular model for plant organisms (The Arabidopsis Genome Initiative, 2000). We chose to grow *R. sativus* because of its particular anatomical distinction between above- and below-ground tissues (Jahren et al., 2008; Schubert and Jahren, 2011), which allowed for clear separation and analysis of root versus shoot and leaf tissues; *R. sativus* is also considered a model species for the study of below-ground growth and root development (e.g., Idso et al., 1988; Idso and Kimball, 1989; Kostka-Rick and Manning, 1993). The number of plants grown at each $p\text{CO}_2$ level ($n = 16$, *R. sativus*; $n = 9$, *A. thaliana*) exceeded the commonly suggested number ($n = 8$) arising from the median number of plants harvested in 350 previous elevated- CO_2 experiments (Poorter and Navas, 2003). Prior to growth within chambers, *R. sativus* seeds (Harris Seeds of Rochester, ID #0071) were germinated on damp paper in the dark under ambient $p\text{CO}_2$ for 5 days, after which they were transferred into standard potting soil (Miracle-Gro Moisture Control) and grown for 29 days within the Plexiglass growth chambers; *A. thaliana* seeds (Columbia, Col-0; Lehle Seeds) were grown from seed to maturity (22 days) within the growth chambers. The experiment length for each species was designed to capture maximum growth prior to the initiation of reproduction based on our previous observations of flowering time.

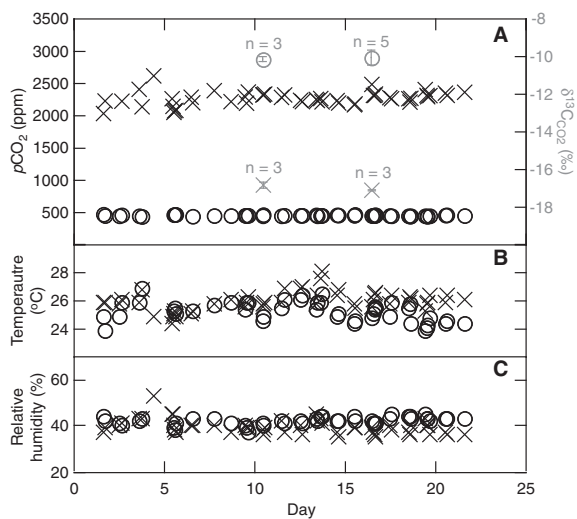


Fig. 1. Examples of the daytime stability of environmental conditions within growth chambers: $p\text{CO}_2$ and $\delta^{13}\text{C}_{\text{CO}_2}$ (A), temperature (B), and relative humidity (C) for ambient (circles) and elevated (crosses) $p\text{CO}_2$ chambers. The mean and standard deviation of the chamber conditions for all experiments are presented in Tables EA1-EA2. $\delta^{13}\text{C}_{\text{CO}_2}$ data are reported as the average and standard deviation for multiple $\delta^{13}\text{C}_{\text{CO}_2}$ measurements made throughout the day.

2.2. Stable isotope analyses

The carbon isotope composition of the CO₂ within each chamber ($\delta^{13}\text{C}_{\text{CO}_2}$) was measured at least six times throughout the growth period using a direct-injection method based on Fry et al. (1996). For this method, chamber air was drawn into a gas-tight syringe and directly introduced into the injector port of a modified Eurovector EA3000 automated combustion system (Eurovector SpA, Milan, Italy). Water vapor was removed using a magnesium perchlorate trap. CO₂ gas was then frozen into a liquid N₂ cold trap, while noncondensable gases were vented to atmosphere. The frozen CO₂ was then thawed at room temperature and passed through a copper reduction column (held at 600 °C) to reduce nitrous oxides to N₂ gas; pure CO₂ gas, within a continuous flow of helium, was diverted to an IsoPrime Isotope Ratio Mass Spectrometer (IRMS) (Micro-mass UK Ltd., Manchester, UK) for carbon isotope analysis. Two reference gases were calibrated *via* dual inlet ($\delta^{13}\text{C} = -10.25\text{‰}$ and -19.4‰ ; 99.995% pure cylinder CO₂; Airgas-Gaspro, Honolulu, USA), and normalized to Vienna Pee Dee Formation limestone (VPDB, $R = {}^{13}\text{C}/{}^{12}\text{C} = 0.011224$) using a two-point curve constructed from CO₂ gas generated from NBS-19 calcium carbonate ($\delta^{13}\text{C}$ consensus value = 1.95‰) and LSVEC lithium carbonate ($\delta^{13}\text{C}$ consensus value = -46.6‰) (Coplen et al., 2006) *via* reaction with 100% H₃PO₄ (Brand et al., 2009). For sample analysis, each CO₂ reference gas stream was diluted with N₂ gas to obtain CO₂ concentrations comparable to chamber air samples. The diluted reference gas was then drawn into an airtight syringe and injected into the direct injection port. Each reference gas was injected after every three sample-injections. Precision for both reference injections and sample injections was better than 0.1‰ (1σ).

Because accurate $\delta^{13}\text{C}_{\text{CO}_2}$ measurements were critical to our analysis, the direct-injection measurements described above were replicated and confirmed by using a second, well-established method for isolating CO₂ for measurement *via* dual inlet. First, chamber air was collected within pre-evacuated, 250-cm³, glass vessels. The CO₂ was then cryogenically isolated, concentrated, and purified from the collected air by slowly bleeding the air sample through a vacuum manifold immersed in an ethanol/liquid-nitrogen trap to remove water, and then through a series of liquid-nitrogen cooled traps to trap CO₂ while simultaneously pumping away noncondensable gases. Any N₂O was removed by heating the cryogenically-purified CO₂ with 0.5 g of reduced copper at 450 °C for 2 h in order to produce copper(II) oxide and N₂ gas. The pure CO₂ sample gas was then analyzed for the $\delta^{13}\text{C}_{\text{CO}_2}$ value *via* the dual inlet of the IsoPrime IRMS. Sample data were normalized to VPDB using a two-point normalization curve constructed from CO₂ gas generated from NBS-19 and LSVEC (Coplen et al., 2006) *via* reaction with 100% H₃PO₄ (Brand et al., 2009). For quality assurance, we analyzed NBS-18 ($\delta^{13}\text{C}$ consensus value = -5.01‰) (Coplen et al., 2006) and MZ calcite ($\delta^{13}\text{C} = -13.30\text{‰}$, calibrated previously within our lab using NBS-19 and LSVEC) within the same batch run as NBS-19, LSVEC, and our samples. Precision for all com-

pounds was better than 0.05‰ (1σ), and all NBS-18 quality assurance samples were within 0.1‰ of their accepted value. We found no significant difference (i.e., $<0.05\text{‰}$) between $\delta^{13}\text{C}_{\text{CO}_2}$ values gained using direct-injection *versus* cryogenic-isolation methods.

At the end of the growth period (29 days for *R. sativus*; 22 days for *A. thaliana*), plants were harvested and above- and below-ground tissues were separated using a razor blade. Tissues were then dried at 60 °C before being ground into a uniform powder using a mortar and pestle in preparation for stable isotope analyses. The $\delta^{13}\text{C}$ values of plant tissues were analyzed using a Delta V Advantage IRMS (Thermo Fisher, Bremen, Germany) coupled to a Costech ECS 4010 Elemental Analyzer with a zero-blank autosampler (Costech Analytical, Valencia, CA, USA). For *R. sativus*, both above- and below-ground tissues were analyzed; only above-ground tissues of *A. thaliana* were analyzed. All samples were introduced to the combustion system in pure tin capsules and measured in triplicate. Within each batch run, the samples were analyzed with two internal lab reference materials that were used to normalize the data to VPDB (JRICE, a white rice obtained from a supermarket and homogenized with a ball mill, $\delta^{13}\text{C} = -27.37\text{‰}$; and JGLY, glycine powder obtained from Fisher Scientific, $\delta^{13}\text{C} = -43.51\text{‰}$). Additionally, a quality assurance sample (JPEP, Bacto Peptone from Becton, Dickinson and Company, $\delta^{13}\text{C} = -14.22\text{‰}$) was incorporated into every batch run and analyzed as an unknown. All three materials (JRICE, JGLY, JPEP) were calibrated within our laboratory and normalized to VPDB using LSVEC and NBS-19, which define the VPDB scale (Coplen et al., 2006). To verify that our calibrations were accurate, we analyzed IAEA-601 benzoic acid (consensus $\delta^{13}\text{C} = -28.81\text{‰}$) (Coplen et al., 2006) as an unknown and obtained $\delta^{13}\text{C} = -28.81 \pm 0.03\text{‰}$ (1σ, $n = 3$). Additionally, we analyzed a C₃₆ *n*-alkane obtained from the Biogeochemistry Laboratory at Indiana University ($\delta^{13}\text{C} = -30.00\text{‰}$) and obtained a value of $-30.00 \pm 0.00\text{‰}$ (1σ, $n = 3$). Over the course of all bulk analyses, the JPEP quality assurance sample returned a mean value of $-14.21 \pm 0.04\text{‰}$ (1σ, $n = 15$), which is in agreement with our calibrated value of -14.22‰ . For tissue samples, the average standard deviation of the three replicate capsules was $<0.05\text{‰}$.

In addition to performing carbon isotope analyses on bulk tissues, we also analyzed untriacontane, an *n*-alkane of chain-length 31 ($n\text{C}_{31}$) from above-ground *R. sativus* tissues following the methods of Bi et al. (2005) and Rommerskirchen et al. (2006). Approximately 160 mg of dried, homogenized plant tissue was ultrasonically extracted with hexane and subsequently isolated by silica gel chromatography using hexane as the mobile phase. In addition, *n*-hexadecane ($n\text{C}_{16}$) was added to each sample for quantitative and isotopic quality control during sample preparation. Urea adduction was carried out in order to remove coextracted species (e.g., squalene, terpenoids, etc.) that might interfere with isotopic analysis. The final solution containing purified *n*-alkanes was dissolved in an appropriate volume of hexane for ~ 70 ng/μL analyte target concentration and 3 μL was injected into an Agilent 6890 Series Gas Chromatograph (Agilent Technologies, Inc., Santa Clara,

USA) equipped with a GC-1 column (25 m × 0.25 mm, 0.25 μm film thickness; GC² Chromatography, Manchester, UK) coupled to the Isoprime IRMS *via* a combustion interface. Identification of nC_{31} was confirmed based on its retention time as determined by multiple analyses of an n -alkane standard mix (Supelco C7-C40 Saturated Alkanes Standard, catalog #49452-U).

We used the following two primary reference materials to normalize our nC_{31} data to VPDB: (1) nC_{36} reference material (obtained from Biogeochemical Laboratories at Indiana University; $\delta^{13}C = -30.00\text{‰}$, verified with our EA, see above) that was co-injected with every sample; and (2) the nC_{16} ($\delta^{13}C = -33.25\text{‰}$) that was added to the bulk material during the n -alkane extraction procedure to allow us to determine n -alkane percent recovery (which exceeded 95%). The nC_{16} internal reference was calibrated using the Indiana University nC_{36} ($C_{36}H_{74}$, $\delta^{13}C = -30.00\text{‰}$), squalene ($C_{30}H_{50}$, $\delta^{13}C = -30.89\text{‰}$), a C_{14} n -alkane ($C_{14}H_{30}$, $\delta^{13}C = -29.66\text{‰}$), and androstane ($C_{19}H_{32}$, $\delta^{13}C = -20.59\text{‰}$), which were all previously characterized offline *via* dual inlet, with accuracy better than 0.1‰. The normalization curve for calibrating the nC_{16} internal reference material was linear with a slope of 0.98.

Normalization curves for correcting the nC_{31} $\delta^{13}C$ data were generated by plotting each primary reference material's raw values against calibrated values. Normalization curve regression slopes fell between 0.98 and 0.99; extrapolation of the normalization curves out to -50‰ could contribute up to 0.5‰ error (based on the minimum and maximum slopes we observed for the normalization curves). Precision (1σ) for the nC_{16} and nC_{31} reference materials was better than 0.1‰ (standard deviations are based on the raw $\delta^{13}C$ values as determined by comparison to the CO₂ reference gas pulses incorporated into every analysis).

In order to verify instrumental linearity out to $\sim -50\text{‰}$, we analyzed one sample (extracted without n -hexadecane) with >90% of the total n -alkanes being comprised of the nC_{31} *via* the online elemental analyzer system, normalizing to VPDB using our internal references JGLY and JRICE. We obtained a value of -49.6‰ , which was 0.3‰ lighter than the nC_{31} compound specific value (-49.3‰), and therefore indicated adequate linearity of our GC analyses across the unusually light n -alkane $\delta^{13}C$ values. All stable isotope values are expressed in the δ-notation in units of per mil (‰).

3. RESULTS

Because the $\delta^{13}C_{CO_2}$ value of the atmosphere we supplied to plants as the raw-material for photosynthesis varied widely ($\delta^{13}C_{CO_2} = -18.0$ to -8.4‰) (Tables EA1-EA2), the range of average $\delta^{13}C$ values measured in the plant tissues grown was also large ($\delta^{13}C_p = -45.2$ to -31.4‰) (Tables EA3-EA4). For *R. sativus*, the $\delta^{13}C_p$ value of above-ground tissue was on average $1.5 \pm 0.5\text{‰}$ depleted relative to the $\delta^{13}C_p$ value of below-ground tissue, consistent with previous results (Badeck et al., 2005; Jahren et al., 2008; Schubert and Jahren, 2011). The $\delta^{13}C_p$ values of nC_{31} -alkanes in *R. sativus* were depleted by $4.8 \pm 0.3\text{‰}$ relative to bulk, above-ground tissue, consistent with other works comparing the carbon isotope composition of bulk-

tissue to isolated specific compounds (Collister et al., 1994; Chikaraishi et al., 2004; Bi et al., 2005; Rommerskirchen et al., 2006).

Although atmospheric pCO_2 affects temperature on the global scale (Cox et al., 2000), we observed no significant relationships between the pCO_2 level and temperature in the *A. thaliana* experiments ($m = 0.0003 \text{ °C ppm}^{-1}$, $R^2 = 0.21$, $P = 0.31$) and the 30 °C ($m = 0.0006 \text{ °C ppm}^{-1}$, $R^2 = 0.30$, $P = 0.13$) and 26 °C ($m = 0.0003 \text{ °C ppm}^{-1}$, $R^2 = 0.15$, $P = 0.30$) *R. sativus* experiments. Similarly, no significant correlations were found between pCO_2 level and relative humidity in any of the experiments (*A. thaliana*, $m = 0.0010\% \text{ ppm}^{-1}$, $R^2 = 0.05$, $P = 0.62$; *R. sativus* warm, $m = 0.0009\% \text{ ppm}^{-1}$, $R^2 = 0.22$, $P = 0.20$; *R. sativus* cool, $m = 0.0005\% \text{ ppm}^{-1}$, $R^2 = 0.07$, $P = 0.49$). The difference between average $\Delta\delta^{13}C_p$ values in *R. sativus* grown at 26 and 30 °C experiments was insignificant ($P = 0.78$; $\Delta\delta^{13}C_{T=30} = 27.2\text{‰}$; $\Delta\delta^{13}C_{T=26} = 27.4\text{‰}$); therefore, we combined the $\Delta\delta^{13}C$ data for these two temperature experiments prior to the analysis of the effect of pCO_2 level on $\Delta\delta^{13}C_p$ values.

All plant tissues analyzed in the study (i.e., above-ground, below-ground, and nC_{31} -alkanes in *R. sativus* and above-ground in *A. thaliana*) showed an increase in carbon isotope discrimination ($\Delta\delta^{13}C$, Eq. (2)) with increasing pCO_2 that closely fitted (i.e., $R \geq 0.94$) the following hyperbolic relationship (Fig. 2):

$$\Delta\delta^{13}C = [(\Delta\delta^{13}C_{\max})(m)(pCO_2 - f)] / [\Delta\delta^{13}C_{\max} + (m) \times (pCO_2 - f)] \quad (3)$$

where $\Delta\delta^{13}C_{\max}$ is the asymptote and m is a measure of the responsiveness. Within these equations, pCO_2 is offset by the value f , such that $\Delta\delta^{13}C = 4.4\text{‰}$ at $pCO_2 = 0$ ppm (after Eq. (1)). Values for $\Delta\delta^{13}C_{\max}$ and m were determined by iterative optimization to minimize the sum of the residuals squared (Schubert and Jahren, 2011). The resulting values for $\Delta\delta^{13}C_{\max}$ ranged across 7.7‰ (26.6–34.3‰) with the highest $\Delta\delta^{13}C_{\max}$ values occurring in nC_{31} -alkanes (*R. sativus*), as expected (Fig. 2). Even among bulk, above-ground tissues $\Delta\delta^{13}C_{\max}$ values were 3‰ higher in *R. sativus* than *A. thaliana* (29.9 versus 26.6‰). The value for m , however, was quite consistent across the different *R. sativus* plant tissues ($m = 0.21$ –0.48), with *A. thaliana* falling within this range ($m = 0.39$) (Fig. 2). Therefore, although there was overall less fractionation measured at each pCO_2 level for *A. thaliana* plants versus *R. sativus* plants, the responsiveness of each species to rising pCO_2 was similar (Fig. 2). In addition, optimization of Eq. (3) to produce a best-fit hyperbola through the combined *A. thaliana* and *R. sativus* datasets results in a strong correlation ($R = 0.82$). This strong correlation and the similarly shaped response to changing pCO_2 level between the two species led us to produce a single equation describing the relationship between $\Delta\delta^{13}C$ and pCO_2 based on the averaged hyperbolic relationships quantified for above-ground tissues of our two model C_3 species:

$$\Delta\delta^{13}C = [(28.26)(0.35)(pCO_2 + 15)] / [28.26 + (0.35) \times (pCO_2 + 15)] \quad (4)$$

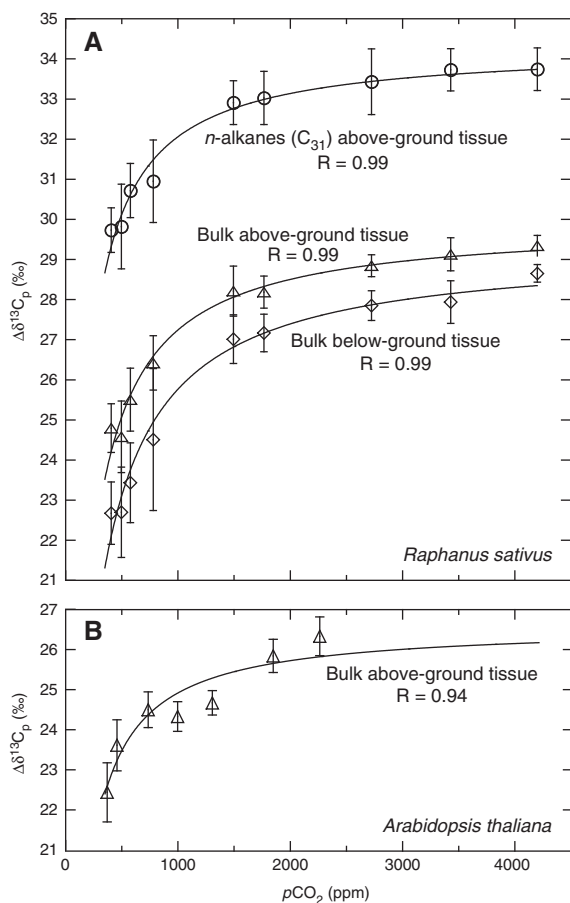


Fig. 2. Influence of $p\text{CO}_2$ on the carbon isotope fractionation of plant tissues ($\Delta\delta^{13}\text{C}_p$, Eq. (2)) for all growth experiments. Data are separated by tissue type and species: (A) *R. sativus* and (B) *A. thaliana*. For all tissues in both species $\Delta\delta^{13}\text{C}_p$ followed an increasing hyperbolic response with increasing $p\text{CO}_2$ (after Eq. (3)): $\Delta\delta^{13}\text{C}_{Raphanus(AG)} = [(29.9)(0.30)(p\text{CO}_2 + 17)] / [29.9 + (0.30)(p\text{CO}_2 + 17)]$; $\Delta\delta^{13}\text{C}_{Raphanus(BG)} = [(29.3)(0.21)(p\text{CO}_2 + 25)] / [29.3 + (0.21)(p\text{CO}_2 + 25)]$; $\Delta\delta^{13}\text{C}_{Raphanus(n31)} = [(34.3)(0.48)(p\text{CO}_2 + 10)] / [34.3 + (0.48)(p\text{CO}_2 + 10)]$ and $\Delta\delta^{13}\text{C}_{Arabidopsis(AG)} = [(26.6)(0.39)(p\text{CO}_2 + 13)] / [26.6 + (0.39)(p\text{CO}_2 + 13)]$.

The nature of the hyperbolic equations requires that $\Delta\delta^{13}\text{C}$ approaches $\Delta\delta^{13}\text{C}_{\text{max}}$ at infinite $p\text{CO}_2$, but in reality, $p\text{CO}_2$ cannot exceed an atmosphere with 100% CO_2 (10^6 ppm). Our hyperbolic equations are consistent with this reality: using the relationship described in Eq. (4), the $\Delta\delta^{13}\text{C}_p$ value calculated at $p\text{CO}_2 = 10^6$ ppm (i.e., a 100% CO_2 atmosphere) differed insignificantly ($<0.01\text{‰}$) from the theoretical maximum value ($\Delta\delta^{13}\text{C}_{\text{max}}$).

4. DISCUSSION

A hyperbolic relationship between plant $\Delta\delta^{13}\text{C}_p$ and $p\text{CO}_2$ has not been previously claimed, although a linear relationship has been reported at low to slightly elevated $p\text{CO}_2$ levels (Feng and Epstein, 1995; Saurer et al., 2003; Sharma and Williams, 2009) and subsequently questioned (McCarroll et al., 2009; Treydte et al., 2009). In order to

compare our measurements with previous work, we surveyed data published between 1994 and 2011 showing a positive response between $\Delta\delta^{13}\text{C}_p$ of vascular C_3 land plants and $p\text{CO}_2$ for at least three different $p\text{CO}_2$ levels (cited with in Table 1). For the published data, the amount of carbon isotope fractionation per unit increase in $p\text{CO}_2$ varied widely ($0.37\text{--}2.70\text{‰}$ $\Delta\delta^{13}\text{C}_p$ per 100 ppm $p\text{CO}_2$) (Table 1). Extrapolation of these relationships implies that $\Delta\delta^{13}\text{C}_p$ values would continue to increase as $p\text{CO}_2$ approaches 10^6 ppm (10^6 ppm) without plateau, reaching values of carbon isotopic discrimination not seen in the current or fossil record of plant life, even for periods when CO_2 concentrations are high [e.g., $\Delta\delta^{13}\text{C}_p = 84.4\text{‰}$ at $p\text{CO}_2 = 4000$ ppm based on the $0.02\text{‰}/\text{ppm}$ increase determined by Feng and Epstein (1995) and $\Delta\delta^{13}\text{C}_p = 4.4\text{‰}$ as c_i/c_a approaches 0 ppm (Farquhar et al., 1989)].

Because our data represent a systematic study at multiple $p\text{CO}_2$ levels ($n = 15$) that span a wide range of partial pressures (370–4200 ppm $p\text{CO}_2$), we have been able to resolve the hyperbolic nature of the relationship between $\Delta\delta^{13}\text{C}_p$ and $p\text{CO}_2$ (Eq. (4)). However, when we plot the amount of fractionation per ppm increase in $p\text{CO}_2$ determined from our data with the published data listed in Table 1, we see that our study is consistent with, and provides a unifying relationship for, previous work on carbon isotopes in plants at elevated $p\text{CO}_2$ (Fig. 3). This is also true upon high-resolution inspection of the relationship between recent and future estimates of $p\text{CO}_2$ (200–800 ppm; Fig. 3 inset). The relationship between the increase in $\Delta\delta^{13}\text{C}_p$ per unit increase in $p\text{CO}_2$ (S) follows a continuous function across $p\text{CO}_2$ (Fig. 3):

$$S = (0.21)(28.26)^2 / [28.26 + 0.21(p\text{CO}_2 + 25)]^2 \quad (5)$$

Eq. (5) ($R = 0.95$) indicates that the increase in $\Delta\delta^{13}\text{C}_p$ associated with increasing $p\text{CO}_2$ approaches zero as the atmosphere becomes saturated with CO_2 . Eq. (5) follows the form of the derivative of our general hyperbolic relationship (Eq. (3)); the integral of Eq. (5) is a hyperbola with the following equation:

$$\Delta\delta^{13}\text{C} = [(28.26)(0.21)(p\text{CO}_2 + 25)] / [28.26 + (0.21) \times (p\text{CO}_2 + 25)] \quad (6)$$

The best-fit curve represented by Eq. (5) was determined iteratively such that Eq. (6) results in $\Delta\delta^{13}\text{C} = 4.4\text{‰}$ at $p\text{CO}_2 = 0$ ppm (after Eq. (1)) and $\Delta\delta^{13}\text{C} = 28.26\text{‰}$ at $p\text{CO}_2 = 10^6$ ppm (after Eq. (4)). We suggest that the wide range of S values reported by previous workers stem from the different $p\text{CO}_2$ levels used in previous experiments ($p\text{CO}_2 = 198\text{--}700$ ppm). Each comparison yielded a unique slope, which presented the appearance of disagreement across results. Here we show that previous estimates were, in fact, correct; the slope of each “linear” response is consistent with the larger pattern (Fig. 3).

An important question is raised by this empirical observation of the effect of $p\text{CO}_2$ on $\Delta\delta^{13}\text{C}_p$: What could be the mechanism by which elevated $p\text{CO}_2$ levels outside of the plant affect the isotopic selectivity that occurs inside the plant? The classic description of carbon isotopic fractionation between plants and the atmosphere upon which most

Table 1
Effects of $p\text{CO}_2$ on $\Delta\delta^{13}\text{C}_p$ as reported in the literature and this study.

S (‰ per 100 ppm)	$p\text{CO}_2$ range (ppm)	Species	References
2.70	198–243	<i>Pinus flexilis</i>	Van de Water et al. (1994)
2.20	243–279	<i>Pinus flexilis</i>	Van de Water et al. (1994)
2.07	303–361	<i>Pinus sylvestris</i>	Berninger et al. (2000)
2.00	300–310	Mixed (11)	Peñuelas and Estiarte (1997)
2.00	277–351	Mixed (4)	Feng and Epstein (1995)
1.88	310–350	Mixed (11)	Peñuelas and Estiarte (1997)
1.75	380–482	<i>Pinus contortus</i>	Sharma and Williams (2009)
1.60	280–380	<i>Sabina przewalskii</i>	Wang et al. (2011)
1.45	285–354	<i>Swietenia macrophylla</i>	Hietz et al. (2005)
1.20	285–365	<i>Juniperus spp.</i>	Treydte et al. (2009)
1.00	343–569	<i>Quercus ilex</i>	Saurer et al. (2003)
0.73	350–700	<i>Quercus petraea</i>	Kürschner et al., (1996)
0.62	380–607	<i>Linaria dalmatica</i>	Sharma and Williams (2009)
0.37	350–700	Mixed (17)	Beerling and Woodward (1995)
0.76	370–455	<i>Arabidopsis thaliana</i>	This study
0.41	455–733	<i>Arabidopsis thaliana</i>	This study
0.20	733–995	<i>Arabidopsis thaliana</i>	This study
0.12	995–1302	<i>Arabidopsis thaliana</i>	This study
0.066	1302–1843	<i>Arabidopsis thaliana</i>	This study
0.039	1843–2255	<i>Arabidopsis thaliana</i>	This study
0.96	407–497	<i>Raphanus sativus</i>	This study
0.72	497–576	<i>Raphanus sativus</i>	This study
0.48	576–780	<i>Raphanus sativus</i>	This study
0.20	780–1494	<i>Raphanus sativus</i>	This study
0.096	1494–1766	<i>Raphanus sativus</i>	This study
0.054	1766–2723	<i>Raphanus sativus</i>	This study
0.029	2723–3429	<i>Raphanus sativus</i>	This study
0.019	3429–4200	<i>Raphanus sativus</i>	This study

Table shows data for studies that measured $\Delta\delta^{13}\text{C}_p$ of C_3 land plants growing under at least three different $p\text{CO}_2$ levels. Studies that found no change or a decrease in $\Delta\delta^{13}\text{C}_p$ with increasing $p\text{CO}_2$ were excluded. When a line or curve was fit to the data, the fitted equation was used to calculate S; S-values are presented here as the increase in $\Delta\delta^{13}\text{C}_p$ per 100 ppm increase in atmospheric CO_2 . S-values reported for this study are for bulk above-ground tissues.

biologists and geologists rely was presented by Vogel (1980) and conceptualized within Farquhar et al. (1989) as Eq. (1) (above). Within this relationship, $p\text{CO}_2$ is represented by the term c_a ; the effect of c_a upon $\Delta\delta^{13}\text{C}_p$ is as the scalar ratio c_i/c_a , which reflects the ratio of $p\text{CO}_2$ inside the leaf (c_i) to $p\text{CO}_2$ outside the leaf (c_a). Stomatal conductance is thought to be the primary control of the ratio c_i/c_a (Farquhar et al., 1989) – so much so that calculation of the c_i/c_a term from the $\Delta\delta^{13}\text{C}_p$ value is commonly used to estimate water-use efficiency in agricultural and ecological studies (Farquhar and Richards, 1984; Farquhar et al., 1988; Ehdaie et al., 1991; Ehleringer et al., 1992; Donovan and Ehleringer, 1994; Rytter, 2005).

In the absence of biochemical experiments, a consideration of the enzymatic activity of RuBisCO (Ribulose-1,5-bisphosphate carboxylase oxygenase) allows us to speculate upon a potential mechanism by which $p\text{CO}_2$ might affect c_i/c_a , entirely independent from the stomata. The role of RuBisCO within the cell is to catalyze the reaction by which a CO_2 molecule is attached to ribulose biphosphate and then shear the resulting molecule into two, three-carbon phosphoglycerate sugars (hence the term “C-3 photosynthesis”). As most of these sugars are recycled back into ribulose biphosphate, one out of every six is used to con-

struct sucrose, which can be transported within the plant for use or storage. Each RuBisCO is a large molecule containing thousands of atoms, organized into 16 separate protein chains. Within each RuBisCO molecule there are eight active sites at which one CO_2 molecule may be attached to one phosphate. At the center of each active site is one magnesium (Mg) atom that must be fully coordinated in order to activate carbon fixation (Walker et al., 1986). Two sites of coordination are supplied by the biphosphate molecule and three are supplied by amino acids that are part of the larger protein chain. The CO_2 molecule to be fixed supplies the final site of coordination, and the reaction proceeds. However, CO_2 molecules play an additional critical role: one of the amino acids required for coordination is a modified form of lysine which can only coordinate with Mg via one CO_2 molecule attached to the end of the lysine side-chain (Hartman et al., 1986). This “activator” CO_2 is required to turn the active site “on” but is not fixed into sugar during the reaction. In a commissioned review, Stitt (1991) suggested that a doubling of $p\text{CO}_2$ would serve to increase sugar production due to the sensitive response of RuBisCO to CO_2 within the cell. We propose that elevated $p\text{CO}_2$ could effectively raise c_i within the cell by supplying the excess CO_2 molecules necessary to coordinate more

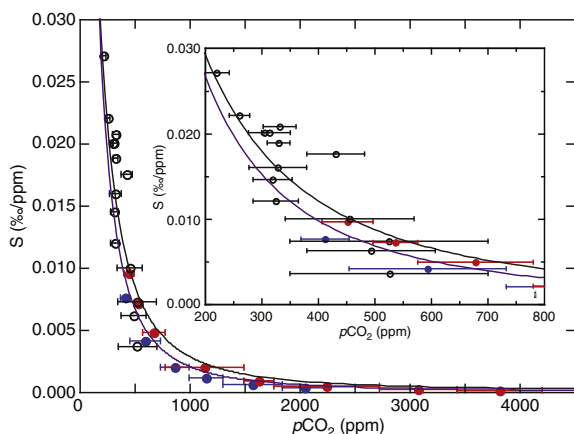


Fig. 3. Plot of the change in carbon isotope fractionation per ppm increase in $p\text{CO}_2$ (S) for C_3 vascular land plants versus $p\text{CO}_2$. Red and blue filled circles reflect our measurements on *R. sativus* and *A. thaliana*, respectively. Open, black circles represent data compiled from published studies that measured plant growth for at least three different $p\text{CO}_2$ levels (data and references are compiled in Table 1). Horizontal bars encompass the range of $p\text{CO}_2$ level variation within each experiment; the circle is plotted at the midpoint of the range. A best-fit function of all the data [black curve; $S = (0.21)(28.26)^2/[28.26 + 0.21(p\text{CO}_2 + 25)]^2$; $R = 0.95$; Eq. (5)] was determined iteratively such that its integral was a hyperbola following the general relationship shown in Eq. (3), with $\Delta\delta^{13}\text{C}$ defined equal to 4.4‰ at $p\text{CO}_2 = 0$ ppm (after Eq. (1)) and $\Delta\delta^{13}\text{C} = 28.26\text{‰}$ at $p\text{CO}_2 = 10^6$ ppm (after Eq. (4)). The purple curve $S = (0.35)(28.26)^2/[28.26 + 0.35(p\text{CO}_2 + 15)]^2$; $R = 0.96$] represents the derivative of Eq. (4), which is based on our *R. sativus* and *A. thaliana* data only. (For interpretation of the references to colour in this figure legend, the reader is referred to the web version of this article.)

Mg atoms within RuBisCO molecules, above and beyond the CO_2 required by fixation and sugar requirements. Under this scenario, a larger proportion of the CO_2 diffused into the leaf is usable for fixation, and c_i is effectively increased relative to c_a . To support this hypothesis, we note that Harley et al. (1992) have modeled increasing intercellular CO_2 concentrations (i.e., c_i) in cotton grown under elevated atmospheric $p\text{CO}_2$ independent of diffusion (Fig. 1 within Harley et al., 1992). As c_i/c_a is effectively increased with increased $p\text{CO}_2$ via this mechanism, $\Delta\delta^{13}\text{C}_p$ increases as predicted by Eq. (1), which is consistent with the hyperbolic relationship we present here (Fig. 2).

In previous work, we observed no significant relationship between $\Delta\delta^{13}\text{C}_p$ and $p\text{CO}_2$ (i.e., Fig. 1 within Arens et al., 2000; Fig. 9 within Jahren et al., 2008). Within these experiments, however, the relative humidity was either unconstrained (Arens et al., 2000) or varied widely both within and between growth experiments (i.e., 14–67%, Fig. 4 within Jahren et al., 2008). Relative humidity has long been recognized to exert strong control over stomatal openness (Raschke, 1976); therefore, it is likely that fluctuations or differences in water vapor deficit influenced c_i/c_a enough to mask the significance of any relationship between $\Delta\delta^{13}\text{C}_p$ and $p\text{CO}_2$. Within the experiments described here, the inherent stability of the external Hawaiian weather (average monthly afternoon relative humidity in Honolulu,

HI = $56 \pm 3\%$, NOAA, 2002) and enhanced control over internal laboratory conditions (Fig. 1C) allowed us to stabilize the water vapor deficit within the chambers such that the isolated effect of $p\text{CO}_2$ on $\Delta\delta^{13}\text{C}_p$ was significant and measurable.

Because the plants in our experiments were grown under conditions of consistently high water availability, we compared $\Delta\delta^{13}\text{C}_p$ values measured in our experiments to those measured in plants grown under wet and humid conditions. For example, many researchers have related modern leaf tissue $\Delta\delta^{13}\text{C}_p$ values to mean annual precipitation (MAP) because precipitation levels affect both soil water status and vapor pressure deficit (Stewart et al., 1995; Schulze et al., 1998; Miller et al., 2001; Warren et al., 2001; Pataki et al., 2003; Hartman and Danin, 2010). Two recent compilations of plant tissues from several biomes confirm a global, positive correlation between $\Delta\delta^{13}\text{C}_p$ and MAP (Diefendorf et al., 2010; Kohn, 2010). Diefendorf et al. (2010) modeled the relationship with a linear regression, while Kohn (2010) states that the relationship “flattens” noticeably at high MAP, consistent with previous observations (Miller et al., 2001). Similarly, an earlier analysis by Warren et al. (2001) found a significant relationship between $\Delta\delta^{13}\text{C}_p$ and MAP for sites with low precipitation and/or high evaporation, but found no such relationship for sites with high precipitation and/or low evaporation. A lack of a correlation between MAP and $\Delta\delta^{13}\text{C}_p$ values for sites with a wide range of very high MAP (2,200 to 5,100 mm/year) has been confirmed by ecologists as well (Schoor and Matson, 2001). In Fig. 4, we plot both Diefendorf et al. (2010) and Kohn (2010) datasets and fit the data to hyperbolic equations, such that $\Delta\delta^{13}\text{C}_p$ will not increase infinitely with increasing MAP (as would result from a linear relationship), but will instead level off in keeping with a more realistic biochemical scenario. From the hyperbolic

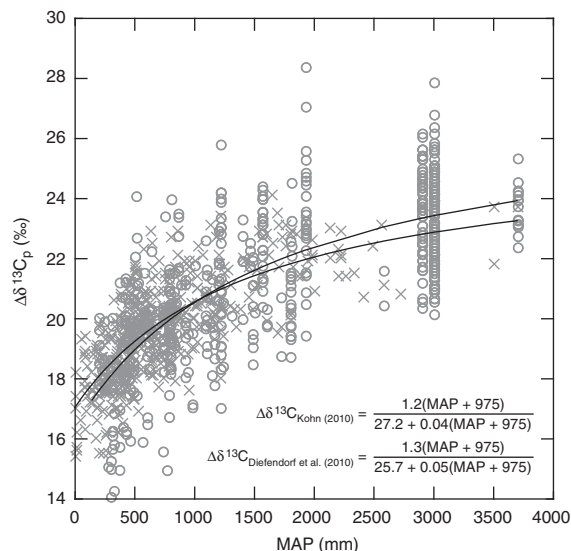


Fig. 4. Influence of mean annual precipitation (MAP) on $\Delta\delta^{13}\text{C}_p$; data compiled by Diefendorf et al., (2010; circles) and Kohn, (2010; crosses). We added best-fit hyperbolic curves to each dataset; both datasets tend toward constant $\Delta\delta^{13}\text{C}_p$ at high MAP.

relationships we applied in Fig. 4, we calculate that above MAP = 2600 mm (Diefendorf et al., 2010) or 2100 mm (Kohn, 2010), increases in $\Delta\delta^{13}\text{C}_p$ are less than 0.1‰ per 100 mm increase in MAP. At these high amounts of MAP, $\Delta\delta^{13}\text{C}_p$ values predicted by the hyperbolic equations in Fig. 4 (22.1‰, Diefendorf et al., 2010; 23.1‰, Kohn, 2010) are commensurate with the $\Delta\delta^{13}\text{C}_p$ values we measured for above-ground tissue at ambient $p\text{CO}_2$ levels (22–24‰) (compare $\Delta\delta^{13}\text{C}_p$ values for sites with MAP above 2100 to 2600 mm in Fig. 4 to $\Delta\delta^{13}\text{C}_p$ values of plants grown under ambient $p\text{CO}_2$ levels (~ 400 ppm) in Fig. 2). Based on these observations, we conclude that the relationships we observed in our growth experiments are consistent with $\Delta\delta^{13}\text{C}_p$ values compiled for plants currently growing in Earth's wettest environments and that the increased fractionation above the $\Delta\delta^{13}\text{C}_p$ values observed under ambient $p\text{CO}_2$ cannot be attributed to stomatal responses to changes in water availability. We note, however, that a change in $p\text{CO}_2$ will cause a change in $\Delta\delta^{13}\text{C}_p$ under any moisture regime.

5. IMPLICATIONS AND CONCLUSIONS

5.1. Calculation of water availability during periods of changing $p\text{CO}_2$

Our evidence for variation in $\Delta\delta^{13}\text{C}_p$ with changes in $p\text{CO}_2$ carries strong implications for the reconstruction of c_i/c_a during periods of elevated or changing atmospheric $p\text{CO}_2$. A plant's efforts to use water efficiently within a given environment are commonly approximated using c_i/c_a values calculated from $\Delta\delta^{13}\text{C}_p$ values (Farquhar et al., 1988; Ehleringer et al., 1992; Donovan and Ehleringer, 1994; Zhang and Marshall, 1994; Brodrick, 1996; Akhter et al., 2003; Cernusak et al., 2007; Golluscio and Oesterheld, 2007) and long-term records of water-use efficiency have been reconstructed from carbon isotopes measured in tree rings (e.g., Feng, 1999; Waterhouse et al., 2004; Gagen et al., 2011). The influence of increased number of active carboxylation sites on RuBisCO with increased $p\text{CO}_2$ that we propose would effectively increase the amount of fixable carbon within the plant, which implies an increase in c_i/c_a (and increase in $\Delta\delta^{13}\text{C}_p$) independent of stomatal function. Thus during periods of increasing $p\text{CO}_2$ (e.g., during Pleistocene glacial to interglacial intervals), increases in $\Delta\delta^{13}\text{C}_p$ values due to increasing $p\text{CO}_2$ could be misinterpreted as evidence of stomatal opening caused by increasingly wet environmental conditions. For illustration, the Vostok ice core records significant increases in $p\text{CO}_2$ of 100 ppm (~ 185 – 285 ppm) every ~ 100 ka over the last 420,000 years (Petit et al., 1999). Using the hyperbolic relationship between $\Delta\delta^{13}\text{C}_p$ and $p\text{CO}_2$ we observed in above-ground tissues of *R. sativus* and *A. thaliana* (Eq. (4)), each of these $p\text{CO}_2$ increases would result in a 2.1‰ increase in $\Delta\delta^{13}\text{C}_p$, independent of any other environmental change. This is in keeping with the actual increase in $\Delta\delta^{13}\text{C}_p$ measured in lumber pine from glacial to non-glacial conditions (15–12 ka) of 2.0‰ (Van de Water et al., 1994). Recent studies, however, have interpreted ecosystem drying or wetting events in the fossil record from changes in the $\Delta\delta^{13}\text{C}_p$

value of fossil plant or terrestrial organic materials, assuming that the same principles apply (e.g., Bowen et al., 2004; Ferrio et al., 2006; Bechtel et al., 2008). We suggest that the isotopic effect of changing atmospheric $p\text{CO}_2$ must be considered before attributing the entirety of any change in the isotopic composition of fossil plant material to changes in the environment, such as water availability.

5.2. Constraint of b -values within Farquhar et al. (1989)

This work also serves to constrain the value of b within Eq. (1), which quantifies the isotopic selectivity for ^{13}C versus ^{12}C assigned to the RuBisCO enzyme. Both the isotopic fractionation due to diffusion and to RuBisCO (a and b within Eq. (1), respectively) are generally conceptualized as constants (Farquhar et al., 1989) and do not depend on CO_2 level (Tcherkez and Farquhar, 2005), but the values for b vary significantly between terrestrial and marine photosynthesizers, and may even vary across different species (Boller et al., 2011). The most commonly invoked values for b in higher plants range between 26 and 30‰ (Christeller et al., 1976; Wong et al., 1979; Farquhar et al., 1982; Roeske and O'Leary, 1984; Guy et al., 1993; Lloyd and Farquhar, 1994; Suits et al., 2005). Eq. (1) requires $b \geq \Delta\delta^{13}\text{C}_p$ because the diffusion of carbon dioxide into plant leaves is a passive process and $p\text{CO}_2$ cannot be concentrated within tissues relative to the atmosphere (i.e., $c_a - c_i$ may not be less than zero and therefore c_i/c_a must not exceed 1). On the basis of our relationship between $\Delta\delta^{13}\text{C}_p$ and $p\text{CO}_2$ for *R. sativus* and *A. thaliana* grown at 370–4200 ppm (Eq. (4)), we see that $\Delta\delta^{13}\text{C}_p$ values approach 28.3‰ at very high $p\text{CO}_2$ levels. Therefore, when the classic relationship proposed by Farquhar et al. (1989) (Eq. (1)) is used to calculate $c_i - c_a$ using $\Delta\delta^{13}\text{C}_p$ values calculated from Eq. (4) for all possible $p\text{CO}_2$ levels, b -values < 28.3 result in $c_i - c_a < 0$ (i.e., $c_i/c_a > 1$) at elevated $p\text{CO}_2$ (Fig. 5), a physiologically impossible scenario. Thus, we propose that b -values for land plants, if constant, must be at least 28.3‰. This result is consistent with the recommendation of Livingston et al. (1999) to use $b = 29$ ‰ based on their results indicating a much better correspondence between the measured and calculated (Eq. (1)) values for c_i/c_a when using $b = 29$ ‰ versus $b = 27$ ‰. We note that our result indicating that b must be at least 28.3‰ is a conservative estimate produced from the average hyperbolic response of two model species; analysis of the *R. sativus* above-ground data alone indicates that b must be at least 29.9‰.

The use of correct b -values is particularly important when making quantitative estimates of water-use efficiency. Water-use efficiency (WUE) has been shown to be proportional to $c_a - c_i$ (Farquhar and Richards, 1984). We show that the assumption of a b value that is too low results in a misinterpretation of WUE under increasing $p\text{CO}_2$. If the value for b used to calculate c_i in Eq. (1) is too low, WUE (and $c_i - c_a$) will appear to increase at low $p\text{CO}_2$, but then decrease at higher $p\text{CO}_2$ levels (Fig. 5). Feng and Epstein (1995) calculated that when c_i/c_a (i.e. $\Delta\delta^{13}\text{C}_p$) increases with increasing $p\text{CO}_2$, water-use efficiency will increase as $p\text{CO}_2$ levels increase for low $p\text{CO}_2$ levels, but

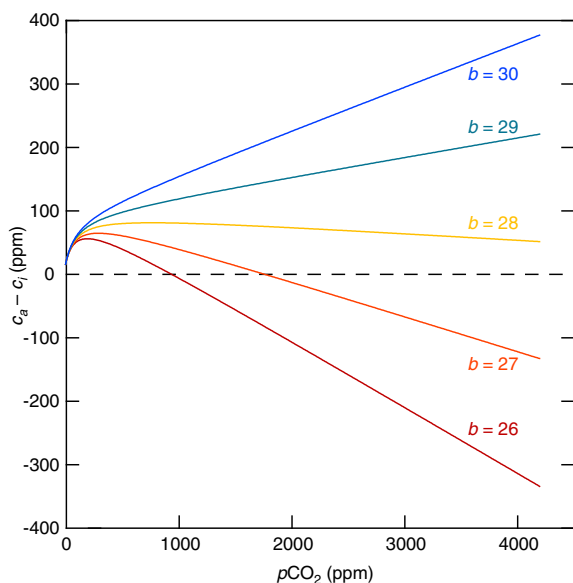


Fig. 5. Relationship between $c_a - c_i$ and $p\text{CO}_2$, as controlled by assumption of commonly invoked b -values ($b = 26\text{--}30\text{‰}$). Values for $c_a - c_i$ were calculated across a large range of $p\text{CO}_2$ levels (i.e., c_a) using Eq. (1) with $\Delta\delta^{13}\text{C}_p$ values calculated from Eq. (4). As $p\text{CO}_2$ increases, b -values $< 28.3\text{‰}$ will yield $c_i > c_a$ (values below the dashed line), which is not physiologically possible.

at high $p\text{CO}_2$ water-use efficiency will decrease with increasing $p\text{CO}_2$. Fig. 5 shows that we can produce a similar, but erroneous change in water-use efficiency if the chosen b -value is too low.

5.3. Correction to tree-ring isotope records based on changing $p\text{CO}_2$

Our work also suggests that a new correction to tree-ring $\delta^{13}\text{C}_p$ records for changing atmospheric $p\text{CO}_2$ is necessary. Carbon isotope records in wood from long-lived trees are generally corrected for the observed changes in $\delta^{13}\text{C}_{\text{CO}_2}$ value (Fig. 6A), but workers have also noted that time-series correlations between climate variables and tree-ring $\delta^{13}\text{C}_p$ values improved when a correction proportional to the increase in $p\text{CO}_2$ was applied (Gagen et al., 2007; Kirilyanov et al., 2008; Loader et al., 2008; Treydte et al., 2009; Wang et al., 2011; Tei et al., 2012). The magnitude of this correction has varied, but has generally been assumed to be linear and equal to $0.007\text{--}0.02 \text{‰}/\text{ppm}$ during the time since the Industrial Revolution (since 1850) (Gagen et al., 2007; Kirilyanov et al., 2008; Treydte et al., 2009; Seftigen et al., 2011; Wang et al., 2011; Kern et al., 2012; Szymczak et al., 2012; Tei et al., 2012). McCarroll et al. (2009) developed a non-linear correction to adjust tree-ring $\delta^{13}\text{C}_p$ records for increasing $p\text{CO}_2$ levels above pre-industrial levels. However, this pre-industrial (“pin”) correction (McCarroll et al., 2009) likely under-corrects $\delta^{13}\text{C}_p$ records that begin after the start of the industrial revolution, which can then affect temperature reconstructions especially for the most recent years (Daux et al., 2011). In contrast to the linear corrections, our results indicate that the depen-

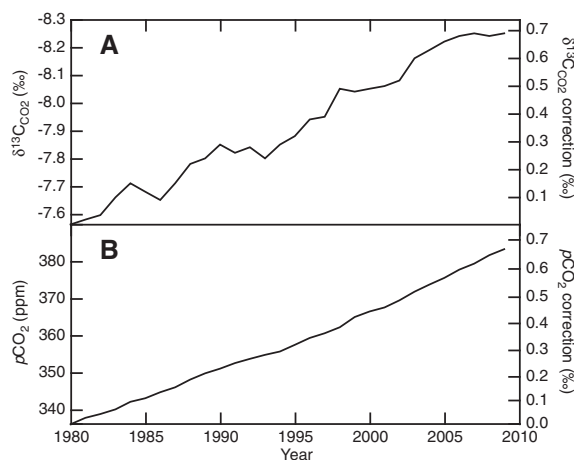


Fig. 6. Comparison of the implied carbon isotope correction due to changes in atmospheric (A) $\delta^{13}\text{C}_{\text{CO}_2}$ and (B) $p\text{CO}_2$ measured at Mauna Loa, Hawaii for the period 1980–2009 (Keeling et al., 2001). Note that the left-hand y-axis in panel (A) is reversed to facilitate comparison of the two corrections. The $p\text{CO}_2$ correction (B, right-hand y-axis) is based on Eq. (6) for the years 1980–2009 (336–383 ppm) and averages $0.023\text{‰}/\text{yr}$ ($0.014\text{‰}/\text{ppm}$).

dence of $\Delta\delta^{13}\text{C}_p$ upon $p\text{CO}_2$ level is best represented hyperbolically (i.e., Eq. (6)), and as $p\text{CO}_2$ levels increase, the amount of carbon isotope fractionation per unit ppm decreases (Fig. 3). Thus, at very high $p\text{CO}_2$ (i.e. $>1800 \text{ ppm}$) we predict little fractionation with changing $p\text{CO}_2$ ($<0.1\text{‰}$ per 100 ppm), while at low $p\text{CO}_2$ (i.e. $<450 \text{ ppm}$) fractionation can be large ($>1\text{‰}$ per 100 ppm) (Eq. (5)). The correction that we suggest based on the $p\text{CO}_2$ rise measured at Mauna Loa during the last thirty years is nearly linear across the relatively small change in $p\text{CO}_2$ from a low value (Fig. 6B). We note that the magnitude of the carbon isotope correction that we suggest due to $p\text{CO}_2$ rise since 1980 is of similar magnitude as the correction for $\delta^{13}\text{C}_{\text{CO}_2}$ caused by the input of ^{13}C -depleted carbon in the forms of fossil fuels and oxidized terrestrial biomass ($\approx 0.7\text{‰}$; Fig. 6).

5.4. Reconstruction of paleo- $p\text{CO}_2$ using the $\Delta\delta^{13}\text{C}_p$ of land-plant specific compounds

The strong ($R = 0.99$) correlation associated with the hyperbolic response of $\Delta\delta^{13}\text{C}_p$ in $n\text{C}_{31}$ -alkanes to changing $p\text{CO}_2$ level (Fig. 2A) raises the possibility of paleo- $p\text{CO}_2$ reconstruction *via* the carbon isotope composition of land-plant specific compounds isolated from the fossil record. Recent successful isolation of long-chain n -alkanes from sedimentary organic matter of Neogene (Feakins et al., 2005; Tipple and Pagani, 2010), Paleogene (van Dongen et al., 2006; Handley et al., 2008; McCarren et al., 2008; Tipple et al., 2011), and Mesozoic (Whiteside et al., 2010; Ruhl et al., 2011) age increase our optimism for the eventual development of such an application. Several important environmental variables, however, would have to be well constrained in order to reconstruct atmospheric $p\text{CO}_2$ from $\delta^{13}\text{C}_p$ with accuracy. Because C_4 photosynthesis employs the pre-concentrating enzyme PEP carboxylase to eliminate

$p\text{CO}_2$ variations in the vicinity of RuBisCO, we do not expect the relationship between $p\text{CO}_2$ and $\Delta\delta^{13}\text{C}_p$ described by Eq. (4) to hold for C_4 plants. However, the expansion of C_4 ecosystems is not thought to have occurred until 5–7 Ma (Cerling et al., 1993), representing a recent phenomenon within the geological record. It is also important to remember that C_4 plants comprise only a small cohort of land plants, largely restricted to desert and grassland environments. Of the 213 major families of Angiosperms, a mere twenty contain C_4 plants (Judd et al., 2007); within the primary C_4 biome of grasslands, the average C_4 contribution is only 36% of the total species (Raven et al., 2004). Desert and grassland paleoenvironments may often be confirmed independently, using palynological and paleosol descriptions (e.g., Kleinert and Strecker, 2001), allowing researchers to disqualify such substrates as appropriate for reconstruction of $p\text{CO}_2$ using the method presented here. We further suggest that changes in the $\delta^{13}\text{C}$ of terrestrial organic material in Neogene sediments preserving ever-wet, non-grassland ecosystems are more likely caused by fluctuations in $p\text{CO}_2$ level than by changes in C_3 versus C_4 plant contribution.

An obvious requirement for this application is an accurate estimate of $\delta^{13}\text{C}_{\text{CO}_2}$ for the time period of interest. Recent successful estimates for Cenozoic $\delta^{13}\text{C}_{\text{CO}_2}$ using a combination of $\delta^{13}\text{C}$ records from benthic and planktonic foraminifera (Tippie et al., 2010) bring us closer to fulfilling this requirement. Second, a substrate that averages the carbon-contribution of several plants under the same conditions is necessary because $\Delta\delta^{13}\text{C}$ values have long been known to vary even among species growing under the same conditions (e.g., Smedley et al., 1991; Marshall and Zhang, 1994; Zhang and Clegg, 1996). This observation has made interpreting environmental conditions such as $\delta^{13}\text{C}_{\text{CO}_2}$ from a $\Delta\delta^{13}\text{C}$ measurement of a single species very difficult (i.e., Arens et al., 2000). This variability has also been well documented in tree ring studies where the $\delta^{13}\text{C}$ value of wood has been shown to vary among species growing within a single site across the same time period (e.g., Leavitt, 2002, 2010). This difference has been attributed to differences in c_i/c_a (Gebrekirstos et al., 2011) or to differences in water transport systems and leaf morphologies (e.g., needle versus broadleaf) (McCarroll and Loader, 2004). For this reason, a substrate that averages the carbon-contribution of several plants under the same conditions is necessary. Therefore, fossilized terrestrial organic matter that contains the contribution of photosynthetic tissues from hundreds of organisms may be a suitable substrate (Jahren and Arens, 2009). Finally, because carbon isotope fractionation in plant tissue is less influenced by water availability across very wet sites compared with drier sites (i.e. $\Delta\delta^{13}\text{C}$ changes very little with increasing precipitation above 2100 mm/yr, Fig. 4), one would need to ensure that the fossilized photosynthetic tissue analyzed was produced under conditions with high water availability. It is encouraging that evidence of past, extremely wet terrestrial environments, such as coal-forming environments, is very common and easily recognized in the fossil record. For example, out of the nearly 4000 terrestrial fossil-sites shown within Scoates (2002) survey, more than half (56%) represent coal-

forming environments. When examining only fossil sites dated to <359 million years, the proportion of sites interpreted as having once been wet environments increases. In addition, certain commonly preserved species are restricted to very wet environments and can be isolated and identified through their leaf or pollen/spore tissues (e.g., the Pteridophyta). To conclude, we suggest that it may be possible to calculate changes in $p\text{CO}_2$ level across critical intervals from the change in $\delta^{13}\text{C}_p$ value of terrestrial plant tissues growing in moist and stable environmental conditions, if atmospheric $\delta^{13}\text{C}_{\text{CO}_2}$ and initial $p\text{CO}_2$ level can be independently estimated.

ACKNOWLEDGEMENTS

We thank H. Cross, A. Ellenson, W.M. Hagopian, G.B. Hunsinger, D.C. King, S. Knutson, G. Kolker, J. McClain, R.J. Panetta, and H. Shelton for laboratory assistance. This work was supported by DOE/BES Grant DE-FG02-09ER16002.

APPENDIX A. SUPPLEMENTARY DATA

Supplementary data associated with this article can be found, in the online version, at <http://dx.doi.org/10.1016/j.gca.2012.08.003>.

REFERENCES

- Ainsworth E. A. and Long S. P. (2005) What have we learned from 15 years of free-air CO_2 enrichment (FACE)? A meta-analytic review of the responses of photosynthesis, canopy properties and plant production to rising CO_2 . *New Phytol.* **165**, 351–372.
- Akhter J., Mahmood K., Tasneem M. A., Naqvi M. H. and Malik K. A. (2003) Comparative water-use efficiency of *Sporobolus arabicus* and *Leptochloa fusca* and its relation with carbon-isotope discrimination under semi-arid conditions. *Plant Soil* **249**, 263–269.
- Andersson N. E. (1991) The influence of constant and diurnally changing CO_2 concentrations on plant-growth and development. *J. Hort. Sci.* **66**, 569–574.
- Arens N. C., Jahren A. H. and Amundson R. (2000) Can C_3 plants faithfully record the carbon isotopic composition of atmospheric carbon dioxide?. *Paleobiology* **26** 137–164.
- Badeck F.-W., Tcherkez G., Nogués S., Piel C. and Ghashghaie J. (2005) Post-photosynthetic fractionation of stable carbon isotopes between plant organs—a widespread phenomenon. *Rapid Commun. Mass Spectrom.* **19**, 1381–1391.
- Bazzaz F. A. (1974) Ecophysiology of *Ambrosia artemisiifolia*: a successional dominant. *Ecology* **55**, 112–119.
- Bazzaz F. A. (1996) *Plants in changing environments*. University Press, Cambridge.
- Bazzaz F. A. and Miao S. L. (1993) Successional status, seed size, and responses of tree seedlings to CO_2 , light, and nutrients. *Ecology* **74**, 104–112.
- Bechtel A., Gratzner R., Sachsenhofer R. F., Gusterhuber J., Lücke A. and Püttmann W. (2008) Biomarker and carbon isotope variation in coal and fossil wood of Central Europe through the Cenozoic. *Palaeogeogr. Palaeoclimatol. Palaeoecol.* **262**, 166–175.
- Beerling D. J. (1996) ^{13}C discrimination by fossil leaves during the late-glacial climate oscillation 12–10 ka BP: measurements and physiological controls. *Oecologia* **108**, 29–37.

- Berling D. J. and Royer D. L. (2002) Fossil plants as indicators of the Phanerozoic global carbon cycle. *Ann. Rev. Earth Planet. Sci.* **30**, 527–556.
- Berling D. J. and Woodward F. I. (1993) Ecophysiological responses of plants to global environmental change since the last glacial maximum. *New Phytol.* **125**, 641–648.
- Berling D. J. and Woodward F. I. (1995) Leaf stable carbon isotope composition records increased water-use efficiency of C₃ plants in response to atmospheric CO₂ enrichment. *Funct. Ecol.* **9**, 394–401.
- Berling D. J., Matthey D. P. and Chaloner W. G. (1993) Shifts in the $\delta^{13}\text{C}$ composition of *Salix herbacea* L. leaves in response to spatial and temporal gradients of atmospheric CO₂ concentration. *Proc. R. Soc. London Ser. B* **253**, 53–60.
- Berner R. A. (2006) GEOCARBSULF: a combined model for Phanerozoic atmospheric O₂ and CO₂. *Geochim. et Cosmochim. Acta* **70**, 5653–5664.
- Berninger F., Sonninen E., Aalto T. and Lloyd J. (2000) Modeling ¹³C discrimination in tree rings. *Global Biogeochem. Cycles* **14**, 213–223.
- Bi X., Sheng G., Liu X., Li C. and Fu J. (2005) Molecular and carbon and hydrogen isotopic composition of *n*-alkanes in plant leaf waxes. *Organ. Geochem.* **36**, 1405–1417.
- Boller A. J., Thomas P. J., Cavanaugh C. M. and Scott K. M. (2011) Low stable carbon isotope fractionation by coccolithophore *RubisCO*. *Geochim. et Cosmochim. Acta* **75**, 7200–7207.
- Bowen G. J., Berling D. J., Koch P. L., Zachos J. C. and Quattlebaum T. (2004) A humid climate state during the Palaeocene/Eocene thermal maximum. *Nature* **432**, 495–499.
- Brand W. A., Huang L., Mukai H., Chivulescu A., Richter J. M. and Rothe M. (2009) How well do we know VPDB? Variability of $\delta^{13}\text{C}$ and $\delta^{18}\text{O}$ in CO₂ generated from NBS19-calcite. *Rapid Commun. Mass Spectrom.* **23**, 915–926.
- Breecker D. O., Sharp Z. D. and McFadden L. D. (2010) Atmospheric CO₂ concentration during ancient greenhouse climates were similar to those predicted for A.D. 2100. *Proc. Natl. Acad. Sci. USA* **107**, 576–580.
- Brodribb T. (1996) Dynamics of changing intercellular CO₂ concentration (c_i) during drought and determination of minimum functional c_i. *Plant Physiol.* **111**, 179–185.
- Cerling T. E., Wang Y. and Quade J. (1993) Expansion of C4 ecosystems as an indicator of global ecological change in the late Miocene. *Nature* **361**, 344–345.
- Cernusak L. A., Aranda J., Marshall J. D. and Winter K. (2007) Large variation in whole-plant water-use efficiency among tropical tree species. *New Phytol.* **173**, 294–305.
- Ceulemans R. and Mousseau M. (1994) Tansley Review No. 71. Effects of elevated atmospheric CO₂ on woody plants. *New Phytol.* **127**, 425–446.
- Chikaraishi Y., Naraoka H. and Poulson S. R. (2004) Carbon and hydrogen isotopic fractionation during lipid biosynthesis in a higher plant (*Cryptomeria japonica*). *Phytochemistry* **65**, 323–330.
- Christeller J. T., Laing W. A. and Troughton J. H. (1976) Isotope discrimination by ribulose 1,5-diphosphate carboxylase: no effect of temperature or HCO₃⁻ concentration. *Plant Physiol.* **57**, 580–582.
- Collister J. W., Rieley G., Stern B., Eglinton G. and Fry B. (1994) Compound-specific $\delta^{13}\text{C}$ analyses of leaf lipids from plants with differing carbon dioxide metabolisms. *Organ. Geochem.* **21**, 619–627.
- Condon M. A., Sasek T. W. and Strain B. R. (1992) Allocation patterns in two tropical vines in response to increased atmospheric carbon dioxide. *Funct. Ecol.* **6**, 680–685.
- Coplen T. B., Brand W. A., Gehre M., Groning M., Meijer H. A. J., Toman B. and Verkouteren R. M. (2006) After two decades a second anchor for the VPDB $\delta^{13}\text{C}$ scale. *Rapid Commun. Mass Spectrom.* **20**, 3165–3166.
- Cox P. M., Betts R. A., Jones C. D., Spall S. A. and Totterdell I. J. (2000) Acceleration of global warming due to carbon-cycle feedbacks in a coupled climate model. *Nature* **408**, 184–187.
- Daux V., Edouard J. L., Masson-Delmotte V., Stievenard M., Hoffmann G., Pierre M., Mestre O., Danis P. A. and Guibal F. (2011) Can climate variations be inferred from tree-ring parameters and stable isotopes from *Larix decidua*? Juvenile effects, budmoth outbreaks, and divergence issue. *Earth Planet. Sci. Lett.* **309**, 221–233.
- Diefendorf A. F., Mueller K. E., Wing S. L., Koch P. L. and Freeman K. H. (2010) Global patterns in leaf ¹³C discrimination and implications for studies of past and future climate. *Proc. Natl. Acad. Sci.* **107**, 5738–5743.
- Donovan L. A. and Ehleringer J. R. (1994) Potential for selection on plants for water-use efficiency as estimated by carbon isotope discrimination. *Am. J. Bot.* **81**, 927–935.
- Downton W. J. S., Grant W. J. R. and Loveys B. R. (1987) Carbon dioxide enrichment increases yield of Valencia orange. *Aust. J. Plant Physiol.* **14**, 493–501.
- Ehdaie B., Hall A. E., Farquhar G. D., Nguyen H. T. and Waines J. G. (1991) Water-use efficiency and carbon isotope discrimination in wheat. *Crop Sci.* **31**, 1282–1288.
- Ehleringer J. R. and Cerling T. E. (1995) Atmospheric CO₂ and the ratio of intercellular to ambient CO₂ concentrations in plants. *Tree Physiol.* **15**, 105–111.
- Ehleringer J. R. and Cooper T. A. (1988) Correlations between carbon isotope ratio and microhabitat in desert plants. *Oecologia* **76**, 562–566.
- Ehleringer J. R., Phillips S. L. and Comstock J. P. (1992) Seasonal variation in the carbon isotopic composition of desert plants. *Funct. Ecol.* **6**, 396–404.
- Farquhar G. D. and Richards R. A. (1984) Isotopic composition of plant carbon correlates with water-use efficiency of wheat genotypes. *Funct. Plant Biol.* **11**, 539–552.
- Farquhar G. D., Ball M. C., von Caemmerer S. and Roksandic Z. (1982) Effect of salinity and humidity on $\delta^{13}\text{C}$ value of halophytes: evidence for diffusional isotope fractionation determined by the ratio of intercellular/atmospheric partial pressure of CO₂ under different environmental conditions. *Oecologia* **52**, 121–124.
- Farquhar G. D., Hubick K. T., Condon A. G. and Richards R. A. (1988) Carbon isotope fractionation and plant water-use efficiency. In *Stable Isotopes in Ecological Research* (eds. P. W. Rundel, J. R. Ehleringer and K. A. Nagy). Springer-Verlag, New York, pp. 21–40.
- Farquhar G. D., Ehleringer J. R. and Hubick K. T. (1989) Carbon isotope discrimination and photosynthesis. *Ann. Rev. Plant Physiol. Plant Mol. Biol.* **40**, 503–537.
- Feakins S. J., deMenocal P. B. and Eglinton T. I. (2005) Biomarker records of late Neogene changes in northeast African vegetation. *Geology* **33**, 977–980.
- Feng X. (1999) Trends in intrinsic water-use efficiency of natural trees for the past 100–200 years: a response to atmospheric CO₂ concentration. *Geochim. et Cosmochim. Acta* **63**, 1891–1903.
- Feng X. and Epstein S. (1995) Carbon isotopes of trees from arid environments and implications for reconstructing atmospheric CO₂ concentration. *Geochim. Cosmochim. Acta* **59**, 2599–2608.
- Ferrio J. P., Alonso N., López J. B., Araus J. L. and Voltas J. (2006) Carbon isotope composition of fossil charcoal reveals aridity changes in the NW Mediterranean Basin. *Global Change Biol.* **12**, 1253–1266.
- Fitter A. H. and Hay R. K. M. (2002) *Environmental Physiology of Plants*, 3rd ed. Academic Press, San Diego.

- Fry B., Garritt R., Tholke K., Neill C., Michener R. H., Mersch F. J. and Brand W. (1996) Cryoflow: cryofocusing nanomole amounts of CO₂, N₂, and SO₂ from an elemental analyzer for stable isotopic analysis. *Rapid Commun. Mass Spectrom.* **10**, 953–958.
- Gagen M., McCarroll D., Loader N. J., Robertson L., Jalkanen R. and Anchukaitis K. J. (2007) Exorcising the 'segment length curse': Summer temperature reconstruction since AD 1640 using non-detrended stable carbon isotope ratios from pine trees in northern Finland. *Holocene* **17**, 435–446.
- Gagen M., Finsinger W., Wagner-Cremer F., McCarroll D., Loader N. J., Robertson I., Jalkanen R., Young G. and Kirchhefer A. (2011) Evidence of changing intrinsic water-use efficiency under rising atmospheric CO₂ concentrations in Boreal Fennoscandia from subfossil leaves and tree ring $\delta^{13}\text{C}$ ratios. *Global Change Biol.* **17**, 1064–1072.
- Gebrekirstos A., van Noordwijk M., Neufeldt H. and Mitlöhner R. (2011) Relationships of stable carbon isotopes, plant water potential and growth: an approach to assess water use efficiency and growth strategies of dry land agroforestry species. *Trees-Struct. Funct.* **25**, 95–102.
- Golluscio R. and Oesterheld M. (2007) Water use efficiency of twenty-five co-existing Patagonian species growing under different soil water availability. *Oecologia* **154**, 207–217.
- Greer D. H., Laing W. A. and Campbell B. D. (1995) Photosynthetic responses of thirteen pasture species to elevated CO₂ and temperature. *Aust. J. Plant Physiol.* **22**, 713–722.
- Gröcke D. R. (1998) Carbon-isotope analyses of fossil plants as a chemostratigraphic and palaeoenvironmental tool. *Lethaia* **31**, 1–13.
- Guy R. D., Fogel M. L. and Berry J. A. (1993) Photosynthetic fractionation of the stable isotopes of oxygen and carbon. *Plant Physiol.* **101**, 37–47.
- Handley L., Pearson P. N., McMillan I. K. and Pancost R. D. (2008) Large terrestrial and marine carbon and hydrogen isotope excursions in a new Paleocene/Eocene boundary section from Tanzania. *Earth Planet. Sci. Lett.* **275**, 17–25.
- Harley P. C., Thomas R. B., Reynolds J. F. and Strain B. R. (1992) Modelling photosynthesis of cotton grown in elevated CO₂. *Plant Cell Environ.* **15**, 271–282.
- Hartman G. and Danin A. (2010) Isotopic values of plants in relation to water availability in the Eastern Mediterranean region. *Oecologia* **162**, 837–852.
- Hartman F. C., Stringer C. D., Milanez S. and Lee E. H. (1986) The active site of Rubisco. *Philos. Trans. R. Soc. B* **313**, 379–395.
- Hietz P., Wanek W. and Dünisch O. (2005) Long-term trends in cellulose $\delta^{13}\text{C}$ and water-use efficiency of tropical *Cedrela* and *Swietenia* from Brazil. *Tree Physiol.* **25**, 745–752.
- Hunt R., Hand D. W., Hannah M. A. and Neal A. M. (1991) Response to CO₂ enrichment in 27 herbaceous species. *Funct. Ecol.* **5**, 410–421.
- Hunt R., Hand D. W., Hannah M. A. and Neal A. M. (1993) Further responses to CO₂ enrichment in British herbaceous species. *Funct. Ecol.* **7**, 661–668.
- Idso S. B. and Kimball B. A. (1989) Growth response of carrot and radish to atmospheric CO₂ enrichment. *Environ. Exp. Bot.* **29**, 135–139.
- Idso S. B., Kimball B. A. and Mauney J. R. (1988) Effects of atmospheric CO₂ enrichment on root:shoot ratios of carrot, radish, cotton and soybean. *Agric. Ecosyst. Environ.* **21**, 293–299.
- Jahren A. H. and Arens N. C. (2009) Prediction of atmospheric $\delta^{13}\text{C}$ using plant cuticle isolated from fluvial sediment: tests across a gradient in salt content. *Palaos* **24**, 394–401.
- Jahren A. H., Arens N. C. and Harbeson S. A. (2008) Prediction of atmospheric $\delta^{13}\text{C}$ using fossil plant tissues. *Rev. Geophys.* **46**, 1–12.
- Judd W. S., Campbell C. S., Kellogg E. A., Stevens P. F. and Donoghue M. J. (2007) *Plant Systematics: A Phylogenetic Approach*, 3rd ed. Sinauer Associates, Sunderland, MA.
- Keeling C. D., Piper S. C., Bacastow R. B., Wahlen M., Whorf T. P., Heimann M. and Meijer H. A. (2001) *Exchanges of Atmospheric CO₂ and ¹³CO₂ with the Terrestrial Biosphere and Oceans from 1978 to 2000. I. Global Aspects*. Scripps Institution of Oceanography, San Diego.
- Kern Z., Patkó M., Kázmér M., Fekete J., Kele S. and Pályi Z. (2012) Multiple tree-ring proxies (earlywood width, latewood width and $\delta^{13}\text{C}$) from pedunculate oak (*Quercus robur* L.), Hungary. *Quat. Int.* <http://dx.doi.org/10.1016/j.quaint.2012.1005.1037>.
- Kimball B. A., Mauney J. R., Nakamura H. and Idso S. B. (1993) Effects of increasing atmospheric CO₂ on vegetation. *Vegetatio* **104**(105), 65–75.
- Kipp E. (2008) Heat stress effects on growth and development in three ecotypes of varying latitude of *Arabidopsis*. *Appl. Ecol. Environ. Res.* **6**, 1–14.
- Kirdyanov A. V., Treydte K. S., Nikolaev A., Helle G. and Schleser G. H. (2008) Climate signals in tree-ring width, density and $\delta^{13}\text{C}$ from larches in Eastern Siberia (Russia). *Chem. Geol.* **252**, 31–41.
- Kleinert K. and Strecker M. R. (2001) Climate change in response to orographic barrier uplift: Paleosol and stable isotope evidence from the late Neogene Santa María basin, northwestern Argentina. *Geol. Soc. Am. Bull.* **113**, 728–742.
- Kohn M. J. (2010) Carbon isotope compositions of terrestrial C3 plants as indicators of (paleo)ecology and (paleo)climate. *Proc. Natl. Acad. Sci.* **107**, 19691–19695.
- Körner C., Farquhar G. D. and Wong S. C. (1991) Carbon isotope discrimination by plants follows latitudinal and altitudinal trends. *Oecologia* **88**, 30–40.
- Kostka-Rick R. and Manning W. J. (1993) Radish (*Raphanus sativus* L.): a model for studying plant responses to air pollutants and other environmental stresses. *Environ. Pollut.* **82**, 107–138.
- Kürschner W. M., van der Burgh J., Visscher H. and Dilcher D. L. (1996) Oak leaves as biosensors of late neogene and early pleistocene paleoatmospheric CO₂ concentrations. *Mar. Micro-paleontol.* **27**, 299–312.
- Leavitt S. W. (2002) Prospects for reconstruction of seasonal environment from tree-ring $\delta^{13}\text{C}$: baseline findings from the Great Lakes area. *USA. Chem. Geol.* **192**, 47–58.
- Leavitt S. W. (2010) Tree-ring C–H–O isotope variability and sampling. *Sci. Total Environ.* **408**, 5244–5253.
- Li P., Ainsworth E. A., Leakey A. D. B., Ulanov A., Lozovaya V., Ort D. R. and Bohnert H. J. (2008) *Arabidopsis* transcript and metabolite profiles: ecotype-specific responses to open-air elevated [CO₂]. *Plant Cell Environ.* **31**, 1673–1687.
- Lin G. and Sternberg L. S. L. (1992) Effect of growth form, salinity, nutrient and sulfide on photosynthesis, carbon isotope discrimination and growth of red mangrove (*Rhizophora mangle* L.). *Aust. J. Plant Physiol.* **19**, 509–517.
- Livingston N. J., Guy R. D., Sun Z. J. and Ethier G. J. (1999) The effects of nitrogen stress on the stable carbon isotope composition, productivity and water use efficiency of white spruce (*Picea glauca* (Moench) Voss) seedlings. *Plant Cell Environ.* **22**, 281–289.
- Lloyd J. and Farquhar G. D. (1994) ^{13}C discrimination during CO₂ assimilation by the terrestrial biosphere. *Oecologia* **99**, 201–215.
- Loader N. J., Santillo P. M., Woodman-Ralph J. P., Rolfe J. E., Hall M. A., Gagen M., Robertson I., Wilson R., Froyd C. A.

- and McCarroll D. (2008) Multiple stable isotopes from oak trees in southwestern Scotland and the potential for stable isotope dendroclimatology in maritime climatic regions. *Chem. Geol.* **252**, 62–71.
- Marshall J. D. and Zhang J. (1994) Carbon isotope discrimination and water-use efficiency in native plants of the north-central Rockies. *Ecology* **75**, 1887–1895.
- Martin B., Bytnerowicz A. and Thorstenson Y. R. (1988) Effects of air pollutants on the composition of stable carbon isotopes, $\delta^{13}\text{C}$, of leaves and wood, and on leaf injury. *Plant Physiol.* **88**, 218–223.
- McCarren H., Thomas E., Hasegawa T., Rhl U. and Zachos J. C. (2008) Depth dependency of the Paleocene-Eocene carbon isotope excursion: paired benthic and terrestrial biomarker records (Ocean Drilling Program Leg 208, Walvis Ridge). *Geochem. Geophys. Geosyst.* **9**, Q10008.
- McCarroll D. and Loader N. J. (2004) Stable isotopes in tree rings. *Quat. Sci. Rev.* **23**, 771–801.
- McCarroll D., Gagen M., Loader N. J., Robertson I., Anchukaitis K. J., Los S., Young G. H. F., Jalkanen R., Kirchhefer A. and Waterhouse J. S. (2009) Correction of tree ring stable isotope chronologies for changes in the carbon dioxide content of the atmosphere. *Geochim. et Cosmochim. Acta* **73**, 1539–1547.
- Melillo J. M., Aber J. D. and Muratore J. F. (1982) Nitrogen and lignin control of hardwood leaf litter decomposition dynamics. *Ecology* **63**, 621–626.
- Miller J. M., Williams R. J. and Farquhar G. D. (2001) Carbon isotope discrimination by a sequence of *Eucalyptus* species along a subcontinental rainfall gradient in Australia. *Funct. Ecol.* **15**, 222–232.
- Mousseau M. and Saugier B. (1992) The direct effect of increased carbon dioxide on gas exchange and growth of forest tree species. *Exp. Bot.* **43**, 1121–1130.
- NOAA 2002, Average Relative Humidity: <http://lwf.ncdc.noaa.gov/oa/climate/online/ccd/avgrh.html> (November 2011).
- Norby R. J., Cotrufo M. F., Ineson P., O'Neill E. G. and Canadell J. G. (2001) Elevated CO_2 , litter chemistry, and decomposition: a synthesis. *Oecologia* **127**, 153–165.
- Park R. and Epstein S. (1960) Carbon isotope fractionation during photosynthesis. *Geochim. Cosmochim. Acta* **21**, 110–126.
- Pataki D. E., Ehleringer J. R., Flanagan L. B., Yakir D., Bowling D. R., Still C. J., Buchmann N., Kaplan J. O. and Berry J. A. (2003) The application and interpretation of Keeling plots in terrestrial carbon cycle research. *Global Biogeochem. Cycles* **17**, 1022.
- Peñuelas J. and Estiarte M. (1997) Trends in plant carbon concentration and plant demand for N throughout this century. *Oecologia* **109**, 69–73.
- Petit J. R., Jouzel J., Raynaud D., Barkov N. I., Barnola J. M., Basile I., Bender M., Chappellaz J., Davis J., Delaygue G., Delmotte M., Kotlyakov V. M., Legrand M., Lipenkov V., Lorius C., Pépin L., Ritz C., Saltzman E. and Stievenard M. (1999) Climate and atmospheric history of the past 420,000 years from the Vostok ice core, Antarctica. *Nature* **399**, 429–436.
- Poorter H. (1993) Interspecific variation in the growth response of plants to an elevated ambient CO_2 concentration. *Vegetatio* **104**(105), 77–97.
- Poorter H. and Navas M.-L. (2003) Plant growth and competition at elevated CO_2 : on winners, losers and functional groups. *New Phytol.* **157**, 175–198.
- Raschke K. (1976) How stomata resolve the dilemma of opposing priorities. *Philos. Trans. R. Soc. B* **273**, 551–560.
- Raven P. H., Evert R. F. and Eichhorn S. E. (2004) *Biology of Plants*, 7th ed. Freeman, W. H.
- Roeske C. A. and O'Leary M. H. (1984) Carbon isotope effects on the enzyme-catalyzed carboxylation of ribulose biphosphate. *Biochemistry* **23**, 6275–6284.
- Rommerskirchen F., Plader A., Eglinton G., Chikaraishi Y. and Rullkötter J. (2006) Chemotaxonomic significance of distribution and stable carbon isotopic composition of long-chain alkanes and alkan-1-ols in C4 grass waxes. *Organ. Geochem.* **37**, 1303–1332.
- Royer D. L. (2001) Stomatal density and stomatal index as indicators of paleoatmospheric CO_2 concentration. *Rev. Palaeobot. Palynol.* **114**, 1–28.
- Ruhl M., Bonis N. R., Reichart G.-J., Damsté J. S. S. and Kürschner W. M. (2011) Atmospheric carbon injection linked to end-Triassic mass extinction. *Science* **333**, 430–434.
- Rytter R. M. (2005) Water use efficiency, carbon isotope discrimination and biomass production of two sugar beet varieties under well-watered and dry conditions. *J. Agron. Crop Sci.* **191**, 426–438.
- Saurer M., Cherubini P., Bonani G. and Siegwolf R. (2003) Tracing carbon uptake from a natural CO_2 spring into tree rings: an isotope approach. *Tree Physiol.* **23**, 997–1004.
- Savard M. M. (2010) Tree-ring stable isotopes and historical perspectives on pollution – An overview. *Environ. Pollut.* **158**, 2007–2013.
- Schleser G. H., Helle G., Lücke A. and Vos H. (1999) Isotope signals as climate proxies: the role of transfer functions in the study of terrestrial archives. *Quat. Sci. Rev.* **18**, 927–943.
- Schubert B. A. and Jahren A. H. (2011) Fertilization trajectory of the root crop *Raphanus sativus* across atmospheric $p\text{CO}_2$ estimates of the next 300 years. *Agr. Ecosys. Environ.* **140**, 174–181.
- Schulze E.-D., Williams R. J., Farquhar G. D., Schulze W., Langridge J., Miller J. M. and Walker B. H. (1998) Carbon and nitrogen isotope discrimination and nitrogen nutrition of trees along a rainfall gradient in northern Australia. *Funct. Plant Biol.* **25**, 413–425.
- Schuur E. and Matson P. (2001) Net primary productivity and nutrient cycling across a mesic to wet precipitation gradient in Hawaiian montane forest. *Oecologia* **128**, 431–442.
- Scotese C. R. (2002) PALEOMAP Project: <http://www.scotese.com/climate.htm> (September 2011).
- Seftigen K., Linderholm H. W., Loader N. J., Liu Y. and Young G. H. F. (2011) The influence of climate on $^{13}\text{C}/^{12}\text{C}$ and $^{18}\text{O}/^{16}\text{O}$ ratios in tree ring cellulose of *Pinus sylvestris* L. growing in the central Scandinavian Mountains. *Chem. Geol.* **286**, 84–93.
- Sharma S. and Williams D. G. (2009) Carbon and oxygen isotope analysis of leaf biomass reveals contrasting photosynthetic responses to elevated CO_2 near geologic vents in Yellowstone National Park. *Biogeosciences* **6**, 25–31.
- Smedley M. P., Dawson T. E., Comstock J. P., Donovan L. A., Sherrill D. E., Cook C. S. and Ehleringer J. R. (1991) Seasonal carbon isotope discrimination in a grassland community. *Oecologia* **85**, 314–320.
- Soil Survey Staff, Soil Conservation Service (1999) *Keys to Soil Taxonomy*. Pocahontas Press, Inc., VA.
- Stewart G. R., Turnbull M. H., Schmidt S. and Erskine P. D. (1995) ^{13}C natural abundance in plant communities along a rainfall gradient: a biological integrator of water availability. *Aust. J. Plant Physiol.* **22**, 51–55.
- Stitt M. (1991) Rising CO_2 levels and their potential significance for carbon flow in photosynthetic cells. *Plant Cell Environ.* **14**, 741–762.
- Suits N. S., Denning A. S., Berry J. A., Still C. J., Kaduk J., Miller J. B. and Baker I. T. (2005) Simulation of carbon isotope

- discrimination of the terrestrial biosphere. *Global Biogeochem. Cycles* **19**.
- Szymczak S., Joachimski M. M., Bräuning A., Hetzer T. and Kuhlemann J. (2012) Are pooled tree ring $\delta^{13}\text{C}$ and $\delta^{18}\text{O}$ series reliable climate archives? – a case study of *Pinus nigra* spp. *laricio* (Corsica/France). *Chemical Geology*. <http://dx.doi.org/10.1016/j.chemgeo.2012.03.013>.
- Tcherkez G. and Farquhar G. D. (2005) Carbon isotope effect predictions for enzymes involved in the primary carbon metabolism of plant leaves. *Funct. Plant Biol.* **32**, 277–291.
- Tcherkez G. G. B., Farquhar G. D. and Andrews T. J. (2006) Despite slow catalysis and confused substrate specificity, all ribulose biphosphate carboxylases may be nearly perfectly optimized. *Proc. Natl. Acad. Sci. U. S. A.* **103**, 7246–7251.
- Tei S., Sugimoto A., Yonenobu H., Hoshino Y. and Maximov T. C. (2012) Reconstruction of summer Palmer Drought Severity Index from $\delta^{13}\text{C}$ of larch tree rings in East Siberia. *Quat. Int.* <http://dx.doi.org/10.1016/j.quaint.2012.1006.1040>.
- The Arabidopsis Genome Initiative (2000) Analysis of the genome sequence of the flowering plant *Arabidopsis thaliana*. *Nature* **408**, 796–815.
- Tipple B. J. and Pagani M. (2010) A 35 Myr North American leaf-wax compound-specific carbon and hydrogen isotope record: implications for C_4 grasslands and hydrologic cycle dynamics. *Earth Planet. Sci. Lett.* **299**, 250–262.
- Tipple B. J., Meyers S. R. and Pagani M. (2010) Carbon isotope ratio of Cenozoic CO_2 : a comparative evaluation of available geochemical proxies. *Paleoceanography* **25**.
- Tipple B. J., Pagani M., Krishnan S., Dirghangi S. S., Galeotti S., Agnini C., Giusberti L. and Rio D. (2011) Coupled high-resolution marine and terrestrial records of carbon and hydrologic cycles variations during the Paleocene-Eocene Thermal Maximum (PETM). *Earth Planet. Sci. Lett.* **311**, 82–92.
- Treydte K. S., Frank D. C., Saurer M., Helle G., Schleser G. H. and Esper J. (2009) Impact of climate and CO_2 on a millennium-long tree-ring carbon isotope record. *Geochim. et Cosmochim. Acta* **73**, 4635–4647.
- Van de Water P. K., Leavitt S. W. and Betancourt J. L. (1994) Trends in stomatal density and $^{13}\text{C}/^{12}\text{C}$ ratios of *Pinus flexilis* needles during last glacial–interglacial cycle. *Science* **264**, 239–243.
- van Dongen B. E., Talbot H. M., Schouten S., Pearson P. N. and Pancost R. D. (2006) Well preserved Palaeogene and Cretaceous biomarkers from the Kilwa area, Tanzania. *Organ. Geochem.* **37**, 539–557.
- Vogel J.C. (1980) Fractionation of the carbon isotopes during photosynthesis. In *Sitzungsberichte der Heidelberger Akademie der Wissenschaften*. Springer-Verlag, Berlin. pp. 111–135.
- Walker D. A., Leegood R. C. and Sivak M. N. (1986) Ribulose biphosphate carboxylase-oxygenase: Its role in photosynthesis. *Philos. Trans. R. Soc. B* **313**, 305–324.
- Ward S. J. E., Midgley G. F., Jones M. H. and Curtis P. S. (1999) Responses of wild C_4 and C_3 grass (Poaceae) species to elevated atmospheric CO_2 concentration: a meta-analytic test of current theories and perceptions. *Global Change Biol.* **5**, 723–741.
- Wang W., Liu X., Shao X., Leavitt S., Xu G., An W. and Qin D. (2011) A 200 year temperature record from tree ring $\delta^{13}\text{C}$ at the Qaidam Basin of the Tibetan Plateau after identifying the optimum method to correct for changing atmospheric CO_2 and $\delta^{13}\text{C}$. *J. Geophys. Res.* **116**, G04022.
- Warren C. R., McGrath J. F. and Adams M. A. (2001) Water availability and carbon isotope discrimination in conifers. *Oecologia* **127**, 476–486.
- Waterhouse J. S., Switsur V. R., Barker A. C., Carter A. H. C., Hemming D. L., Loader N. J. and Robertson I. (2004) Northern European trees show a progressively diminishing response to increasing atmospheric carbon dioxide concentrations. *Quat. Sci. Rev.* **23**, 803–810.
- Whiteside J. H., Olsen P. E., Eglinton T., Brookfield M. E. and Sambrotto R. N. (2010) Compound-specific carbon isotopes from Earth's largest flood basalt eruptions directly linked to the end-Triassic mass extinction. *Proc. Natl. Acad. Sci. U. S. A.* **107**, 6721–6725.
- Wong W. W., Benedict C. R. and Kohel R. J. (1979) Enzymic fractionation of the stable carbon isotopes of carbon dioxide by ribulose-1,5-bisphosphate carboxylase. *Plant Physiol.* **63**, 852–856.
- Woodward F. I. (1987) Stomatal numbers are sensitive to increases in CO_2 from pre-industrial levels. *Nature* **327**, 617–618.
- Woodward F. I. and Bazzaz F. A. (1988) The responses of stomatal density to CO_2 partial pressure. *J. Exp. Bot.* **39**, 1771–1781.
- Woodward F. I. and Kelly C. K. (1995) The influence of CO_2 concentration on stomatal density. *New Phytol.* **131**, 311–327.
- Zhang J. and Marshall J. D. (1994) Population differences in water-use efficiency of well-watered and water-stressed western larch seedlings. *Can. J. For. Res.* **24**, 92–99.
- Zhang J. W. and Clegg B. M. (1996) Variation in stable carbon isotope discrimination among and within exotic conifer species grown in eastern Nebraska, USA. *For. Ecol. Manage.* **83**, 181–187.

Associate editor: Martin Novak

Schubert and Jahren – “The effect of atmospheric CO₂ concentration on carbon isotope fractionation in C3 land plants,” Electronic Annex, Tables EA1-EA4.

Table EA1. Elevated $p\text{CO}_2$ experiments performed on *R. sativus*.*

$p\text{CO}_2$ (ppm) [†]	$\delta^{13}\text{C}_{\text{CO}_2}$ (ppm) [†]	Temperature (°C) [†]	Humidity (%) [†]	Water (ml)
407 ± 22	-8.4 ± 0.2	29.5 ± 2.7	32 ± 8	510
407 ± 22	-8.4 ± 0.2	25.5 ± 1.9	41 ± 6	380
497 ± 13	-9.7 ± 0.1	31.4 ± 1.6	36 ± 10	550
497 ± 13	-9.7 ± 0.1	26.7 ± 1.8	41 ± 5	470
576 ± 28	-10.1 ± 0.3	29.1 ± 2.5	32 ± 9	500
576 ± 28	-10.1 ± 0.3	25.8 ± 1.7	36 ± 4	440
780 ± 51	-12.4 ± 0.2	28.7 ± 2.6	31 ± 8	500
780 ± 51	-12.4 ± 0.2	23.9 ± 2.2	39 ± 4	410
1494 ± 97	-15.7 ± 0.3	28.4 ± 3.1	34 ± 9	660
1494 ± 97	-15.7 ± 0.3	24.2 ± 2.7	35 ± 5	550
1766 ± 69	-15.9 ± 0.1	32.2 ± 2.1	40 ± 12	610
1766 ± 69	-15.9 ± 0.1	25.9 ± 3.1	39 ± 4	540
2723 ± 113	-16.7 ± 0.1	31.0 ± 2.3	35 ± 11	560
2723 ± 113	-16.7 ± 0.1	26.0 ± 2.0	38 ± 5	460
3429 ± 180	-16.8 ± 0.1	31.1 ± 1.9	36 ± 10	530
3429 ± 180	-16.8 ± 0.1	26.4 ± 1.7	43 ± 5	420
4200 ± 110	-17.2 ± 0.2	31.7 ± 1.9	36 ± 12	550
4200 ± 110	-17.2 ± 0.2	26.4 ± 2.0	40 ± 5	480
<i>Warm average</i>		<i>30.3 ± 1.4</i>	<i>35 ± 3</i>	<i>552 ± 53</i>
<i>Cool average</i>		<i>25.6 ± 1.0</i>	<i>39 ± 3</i>	<i>461 ± 57</i>

*Eight plants were grown for each set of conditions.

[†]Values are reported as the mean ± 1σ, as measured throughout the 29-day experiment.

Table EA2. Elevated $p\text{CO}_2$ experiments performed on *A. thaliana*.*

$p\text{CO}_2$ (ppm) [†]	$\delta^{13}\text{C}_{\text{CO}_2}$ (‰) [†]	Temperature (°C) [†]	Humidity (%) [†]	Water (ml)
370 ± 17	-9.6 ± 0.1	24.7 ± 1.6	43 ± 3	105
455 ± 13	-10.1 ± 0.4	24.4 ± 1.6	43 ± 3	215
733 ± 18	-13.6 ± 0.1	25.4 ± 1.9	37 ± 5	215
995 ± 80	-14.6 ± 0.1	24.3 ± 1.7	42 ± 5	105
1302 ± 54	-15.4 ± 0.1	24.8 ± 1.6	39 ± 4	220
1843 ± 31	-18.0 ± 0.3	25.2 ± 1.8	46 ± 5	105
2255 ± 148	-17.1 ± 0.1	25.1 ± 1.8	42 ± 6	155
<i>Average</i>		<i>24.8 ± 0.4</i>	<i>42 ± 3</i>	<i>160 ± 56</i>

*Nine plants were grown for each set of conditions.

[†]Values are reported as the mean ± 1σ, as measured throughout the 22-day experiment.

Table EA3. $\delta^{13}\text{C}$ values measured in above-ground (AG) and below-ground (BG) bulk tissues, and *n*-alkanes (n31) for *R. sativus**.

ID	$p\text{CO}_2$ (ppm)	$\delta^{13}\text{C}_{\text{bulk(AG)}}$ (‰)	$\delta^{13}\text{C}_{\text{stdev}}$ (‰)	$\delta^{13}\text{C}_{\text{bulk(BG)}}$ (‰)	$\delta^{13}\text{C}_{\text{stdev}}$ (‰)	$\delta^{13}\text{C}_{\text{n31}}$ (‰)	$\delta^{13}\text{C}_{\text{stdev}}$ (‰)
HH01	407	-33.28	0.02	-31.63	0.02	-37.33	
HH02	407	-32.18	0.02	-30.12	0.01		
HH03	407	-33.24	0.03	-31.26	0.03	-37.87	
HH04	407	-32.44	0.05	-30.61	0.03	-36.87	
HH05	407	-32.82	0.05	-31.17	0.01	-37.37	
HH06	407	-32.23	0.04	-30.14	0.02	-36.30	
HH07	407	-32.04	0.03	-30.08	0.01	-36.91	
HH08	407	-33.22	0.02	-31.19	0.02	-37.20	
HH09	407	-32.07	0.01	-29.56	0.01	-36.90	
HH10	407	-32.39	0.05	-29.89	0.02	-38.01	
HH11	407	-32.38	0.01	-30.42	0.04	-37.02	
HH12	407	-31.23	0.02	-28.82	0.02	-37.15	0.13
HH13	407	-32.47	0.00	-30.75	0.01	-36.61	
HH14	407	-31.78	0.05	-29.84	0.03	-36.96	0.01
HH15	407	-31.69	0.06	-29.73	0.01	-36.08	
HH16	407	-32.50	0.01	-30.67	0.03	-36.56	
C01	497	-32.76	0.04	-31.71	0.10		
C02	497	-32.06	0.10	-29.48	0.03	-36.46	0.17
C03	497	-33.18	0.04	-31.01	0.13	-39.25	0.08
C04	497	-34.36	0.05	-32.43	0.06	-39.49	0.03
C05	497	-32.95	0.06	-31.57	0.05		
C06	497	-32.41	0.05	-30.41	0.16	-37.54	0.07
C07	497	-33.18	0.03	-31.43	0.03	-38.01	0.15
C08	497	-33.39	0.06	-31.26	0.08	-38.03	0.07
C09	497	-34.37	0.05	-32.74	0.03	-38.86	0.05
C10	497	-35.05	0.08	-33.62	0.04	-39.55	0.06
C11	497	-33.92	0.06	-32.29	0.08	-39.27	0.14
C12	497	-32.47	0.09	-30.25	0.05	-37.25	0.00
C13	497	-33.13	0.03	-31.30	0.03	-37.41	0.20
C14	497	-34.26	0.02	-32.70	0.06	-38.91	
C15	497	-33.44	0.04	-31.97	0.05	-38.74	0.05
C16	497	-34.20	0.14	-32.52	0.06		
GG01	576	-34.64	0.03	-32.39	0.01	-39.54	
GG02	576	-35.30	0.06	-33.69	0.03	-39.92	0.09
GG03	576	-34.92	0.05	-32.96	0.04	-39.52	
GG04	576	-34.43	0.01	-32.33	0.03	-39.66	
GG05	576	-34.51	0.04	-33.02	0.02	-39.58	
GG06	576	-35.75	0.13	-33.84	0.04	-39.69	
GG07	576	-33.87	0.05	-31.38	0.02	-39.69	
GG08	576	-35.58	0.02	-34.03	0.02	-39.61	
GG09	576	-34.43	0.03	-32.66	0.02	-39.90	
GG10	576	-33.80	0.09	-31.67	0.06	-39.94	
GG11	576	-33.41	0.00	-31.38	0.05	-37.96	
GG12	576	-35.13	0.12	-33.11	0.01	-39.37	
GG13	576	-34.53	0.08	-31.71	0.02	-39.07	
GG14	576	-34.95	0.04	-33.05	0.03	-39.34	

GG15	576	-36.20	0.03	-34.43	0.01	-41.02	
GG16	576	-34.51	0.06	-33.05	0.03	-40.28	0.08
JJ01	780	-38.41	0.13	-30.70	0.02	-41.79	0.00
JJ02	780	-37.23	0.03	-35.09	0.07	-41.62	
JJ03	780	-37.65	0.05	-36.22	0.04	-41.99	
JJ04	780	-37.70	0.03	-36.46	0.00	-42.06	
JJ05	780	-38.61	0.03	-37.21	0.03		
JJ06	780	-36.73	0.04	-35.19	0.08	-41.19	
JJ07	780	-37.43	0.01	-36.33	0.03		
JJ08	780	-38.21	0.01	-36.91	0.03	-43.12	0.11
JJ09	780	-39.24	0.03	-37.99	0.04	-44.07	
JJ10	780	-37.40	0.04	-35.31	0.05		
JJ11	780	-37.63	0.04	-36.71	0.08	-41.02	
JJ12	780	-38.14	0.01	-36.00	0.02	-43.02	
JJ13	780	-38.05	0.03	-37.07	0.04	-42.17	
JJ14	780	-37.12	0.05	-35.13	0.04	-40.79	
JJ15	780	-37.33	0.06	-36.24	0.01	-41.61	
JJ16	780	-38.09	0.04	-37.66	0.01		
EE01	1494						
EE02	1494	-42.65	0.06	-40.90	0.06	-47.33	
EE03	1494	-42.97	0.05	-41.87	0.10	-47.74	
EE04	1494	-43.26	0.03	-41.89	0.03		
EE05	1494	-42.84	0.07	-41.82	0.04	-46.60	0.10
EE06	1494	-42.84	0.10	-41.18	0.01	-46.99	
EE07	1494	-42.44	0.03	-41.23	0.09	-47.05	0.11
EE08	1494	-41.12	0.04	-40.43	0.02	-45.96	
EE09	1494	-41.70	0.07	-40.62	0.02	-47.82	0.09
EE10	1494	-43.01	0.08	-41.81	0.06	-47.17	
EE11	1494	-43.22	0.05	-42.27	0.02	-46.62	
EE12	1494	-42.79	0.02	-41.82	0.02	-46.89	0.25
EE13	1494	-42.57	0.02	-41.93	0.08		
EE14	1494	-42.46	0.06	-41.44	0.02	-46.93	
EE15	1494	-43.24	0.07	-42.33	0.07	-47.14	
EE16	1494	-42.90	0.11	-41.72	0.03		
D01	1766	-42.88	0.10	-41.91	0.08	-46.73	0.04
D02	1766	-42.60	0.03	-41.58	0.11	-47.29	0.06
D03	1766	-42.81	0.07	-41.30	0.06	-46.98	0.23
D04	1766	-42.79	0.02	-41.72	0.01		
D05	1766	-43.28	0.08	-42.08	0.08	-47.39	0.04
D06	1766	-42.57	0.01	-41.29	0.06	-46.49	
D07	1766	-42.39	0.03	-42.05	0.02	-46.98	0.05
D08	1766	-42.58	0.04	-41.34	0.05	-47.12	0.02
D09	1766	-43.16	0.11	-42.39	0.11	-47.80	0.04
D10	1766					-46.85	0.24
D11	1766	-42.88	0.07	-41.68	0.09	-48.74	0.06
D12	1766	-42.36	0.06	-42.44	0.02	-47.79	0.08
D13	1766	-43.44	0.06	-42.55	0.01	-48.01	0.36
D14	1766	-43.50	0.04	-42.55	0.03		
D15	1766	-42.56	0.02	-41.91	0.03	-47.41	0.03
D16	1766	-43.23	0.01	-42.02	0.04		
A01	2723	-44.39	0.05	-43.15	0.17	-48.13	0.17

A02	2723	-44.41	0.08	-43.25	0.02	-47.33	0.14
A03	2723	-44.33	0.10	-43.63	0.06	-47.92	0.06
A04	2723	-43.97	0.05	-42.68	0.12	-49.28	0.10
A05	2723	-44.29	0.03	-43.51	0.03		
A06	2723	-44.02	0.05	-43.73	0.05	-48.40	0.11
A07	2723	-43.94	0.08	-43.39	0.02	-47.76	0.17
A08	2723	-44.01	0.04	-43.15	0.18	-47.98	0.02
A09	2723	-44.58	0.07	-43.27	0.21	-48.43	0.01
A10	2723	-44.30	0.02	-43.47	0.17	-49.20	0.15
A11	2723	-44.73	0.06	-43.90	0.05	-49.30	0.10
A12	2723	-44.42	0.07	-43.41	0.03	-48.09	0.08
A13	2723	-44.36	0.10	-42.88	0.20	-49.88	0.08
A14	2723	-43.89	0.03	-43.05	0.12		
A15	2723	-44.50	0.06	-43.82	0.11	-49.08	0.02
A16	2723						
E01	3429	-45.17	0.06	-43.97	0.03	-49.31	0.06
E02	3429	-44.39	0.02	-43.67	0.01	-49.34	0.09
E03	3429	-44.43	0.27	-43.74	0.07	-48.60	0.02
E04	3429	-43.99	0.21	-43.22	0.09		
E05	3429	-44.75	0.02	-43.89	0.04	-48.36	0.17
E06	3429	-44.24	0.00	-42.92	0.07	-49.73	0.11
E07	3429	-44.06	0.09	-43.22	0.11	-48.39	0.18
E08	3429	-44.90	0.01	-44.44	0.09	-48.37	0.30
E09	3429	-44.87	0.05	-43.30	0.13	-48.83	0.11
E10	3429	-44.85	0.01	-43.46	0.20	-48.17	0.17
E11	3429	-44.81	0.02	-43.73	0.07	-48.93	0.02
E12	3429	-45.04	0.06	-43.91	0.08		
E13	3429	-44.97	0.06	-43.43	0.29	-48.85	0.17
E14	3429	-44.30	0.12	-42.33	0.09	-49.54	0.02
E15	3429	-45.16	0.02	-43.97	0.16	-49.33	0.20
E16	3429	-44.44	0.07	-43.48	0.05	-49.04	0.10
B01	4200	-45.03	0.07	-44.51	0.06	-48.77	0.13
B02	4200	-45.51	0.02	-44.58	0.05	-48.90	0.02
B03	4200	-45.04	0.10	-43.91	0.08		
B04	4200	-45.35	0.03	-44.66	0.02	-48.72	0.07
B05	4200	-45.56	0.03	-44.75	0.03	-50.23	0.04
B06	4200	-45.40	0.02	-44.53	0.04	-49.32	0.07
B07	4200	-45.16	0.02	-44.42	0.09	-49.71	0.12
B08	4200	-45.18	0.06	-44.74	0.13	-48.41	0.17
B09	4200	-44.93	0.07	-44.61	0.04	-49.31	0.03
B10	4200	-44.94	0.03	-44.66	0.11	-48.94	0.29
B11	4200	-45.14	0.02	-44.52	0.04	-49.17	0.06
B12	4200	-45.34	0.57	-44.75	0.08	-49.36	0.12
B13	4200	-44.78	0.03	-44.71	0.05	-49.88	0.02
B14	4200	-45.04	0.02	-44.55	0.02	-49.37	0.08
B15	4200	-45.22	0.01	-44.40	0.07		
B16	4200	-45.56	0.01	-44.60	0.06	-49.41	0.10

*Reported $\delta^{13}\text{C}$ values for bulk tissues are for triplicate measurements. Due to limited sample material, $\delta^{13}\text{C}_{\text{n31}}$ could not be measured in triplicate for all samples.

Table EA4. $\delta^{13}\text{C}$ values measured in above-ground *A. thaliana* tissues*.

Sample ID	$p\text{CO}_2$ (ppm)	$\delta^{13}\text{C}_{\text{avg}}$ (‰)	$\delta^{13}\text{C}_{\text{stdev}}$ (‰)
E-01-AG	370	-31.55	0.03
E-03-AG	370	-31.69	0.03
E-05-AG	370	-32.52	0.06
E-07-AG	370	-30.49	0.04
E-09-AG	370	-30.97	0.03
E-11-AG	370	-32.18	0.05
E-13-AG	370	-30.78	0.06
E-15-AG	370	-30.67	0.03
E-17-AG	370	-31.43	0.06
A-01-AG	455	-32.58	0.12
A-03-AG	455	-32.51	0.06
A-05-AG	455	-32.85	0.07
A-07-AG	455	-33.83	0.03
A-09-AG	455	-33.20	0.02
A-11-AG	455		
A-13-AG	455	-33.28	0.09
A-15-AG	455	-32.67	0.04
A-17-AG	455	-32.63	0.08
B-01-AG	733	-37.59	0.02
B-03-AG	733	-37.65	0.15
B-05-AG	733	-37.33	0.06
B-07-AG	733	-36.61	0.18
B-09-AG	733	-37.53	0.06
B-11-AG	733		
B-13-AG	733	-36.60	0.06
B-15-AG	733	-37.14	0.06
B-17-AG	733	-37.43	0.19
G-01-AG	995	-38.03	0.04
G-03-AG	995	-37.76	0.04
G-05-AG	995	-38.23	0.04
G-07-AG	995	-37.55	0.02
G-09-AG	995	-38.18	0.04
G-11-AG	995	-38.04	0.00
G-13-AG	995	-37.71	0.12
G-15-AG	995	-38.60	0.03
G-17-AG	995	-38.46	0.01
C-01-AG	1302	-39.17	0.20
C-03-AG	1302	-38.90	0.11
C-05-AG	1302	-38.76	0.08
C-07-AG	1302	-39.25	0.68
C-09-AG	1302	-38.81	0.06
C-11-AG	1302	-39.38	0.12
C-13-AG	1302	-39.14	0.06
C-15-AG	1302	-39.61	0.03
C-17-AG	1302	-39.36	0.03
I-01-AG	1843	-42.78	0.02
I-03-AG	1843	-42.81	0.05
I-05-AG	1843	-42.66	0.04

I-07-AG	1843	-42.88	0.02
I-09-AG	1843	-42.56	0.00
I-11-AG	1843	-42.03	0.06
I-13-AG	1843	-43.15	0.03
I-15-AG	1843	-42.95	0.06
I-17-AG	1843	-43.14	0.06
D-01-AG	2255	-42.79	0.02
D-03-AG	2255	-42.63	0.03
D-05-AG	2255	-42.53	0.02
D-07-AG	2255	-41.63	0.09
D-09-AG	2255	-42.42	0.03
D-11-AG	2255	-42.90	0.08
D-13-AG	2255	-42.05	0.03
D-15-AG	2255	-42.34	0.04
D-17-AG	2255	-41.71	0.07

*Reported $\delta^{13}\text{C}$ values are for triplicate measurements.